A COMPARATIVE ANALYSIS OF TWO THERMOECONOMIC DIAGNOSIS METHODOLOGIES IN A BUILDING HEATING AND DHW FACILITY

Ana Picallo[1], José Mª Sala, Cesar Escudero
Research group ENEDI, Department of Thermal Engineering, University of the Basque Country (UPV/EHU); Alameda Urquijo, S/N, 48013 Bilbao, Vizcaya, Spain.
[1]Corresponding author. E-mail: ana.picallo@ehu.eus

ABSTRACT

Concerning the building environment HVAC facilities, even if a great effort has been made in developing components and systems with high nominal efficiencies, less attention has been paid to the problem of system maintenance.

The main objective of the *thermoeconomic diagnosis* is to detect possible anomalies and their location inside a component of the energy system. The second objective, and indeed the one to be achieved in this paper, is indicated as *inverse problem.* It is associated with the quantification of the effects of anomalies in terms of thermoeconomic quantities. Its rigorous application in building thermal installations has some difficulties relating to the strong interrelation between the different components and the fact that energy supply facilities are continuously changing with time.

The way to deal with *dynamic* circumstances is thoroughly explored in this article.

Likewise, this paper's main goal is to demonstrate an application of two thermoeconomic diagnosis methodologies in the building sector, one based on the *malfunction and dysfunction* analysis and the other one based on the *characteristic curves* of the components. The results obtained allow us to point out the advantages and limitations of both methodologies as well as to combine them and then develop a more reliable diagnosis.

Keywords: Thermoeconomic diagnosis; Dynamic behaviour; Malfunction and Dysfunction; Characteristic curves; Multi-fault.

Highlights: ♦ Detailed dynamic thermoeconomic diagnosis in buildings energy supply system is made ♦ A new way for fault detection and their effects quantification is developed ♦ Two thermoeconomic diagnosis methods are applied ♦ Characteristic curves and MF and DF methods are shown to be complementary ♦ Diagnosis of a multi-fault heating and DHW facility is performed.

1. INTRODUCCTION

In recent years, the construction sector has been in the spotlight of policies focusing on the reduction of primary energy consumption and also oriented in the downsizing of CO_2 emissions. It is estimated that heating, ventilation and air conditioning (HVAC) systems consume about 50% of the total energy used in buildings worldwide. Then by properly operating the HVAC systems, considerable energy savings can be achieved [1].

However, it is not only a matter of designing and sizing the higher performance thermal systems, optimizing its costs and trying to design them for the minimum environmental impact, since its *maintenance* should also be taken into consideration.

Systems are often poorly maintained and experience dramatic degradation of performance due to aging and the presence of malfunctions or faults [2]. Those anomalies do not cause the unit to stop functioning, but they do produce degradation in plant performance that could be the beginning of undesirable induced effects which can seriously damage the nominal operational condition of the facility.

Thermoeconomic diagnosis is focused on discovering reductions in system efficiency, the detection of possible anomalies, the identification of the components where these anomalies have occurred and their quantification [3]. This paper compares two thermoeconomic methodologies in the diagnosis of a heating and DHW supply system, one based on the malfunction and dysfunction method [4] and the other one based on the characteristic curves [5] of the components.

The paper is organized in 6 different sections as follows: after the introductory first section, Section 2 presents the main ideas and sums up the malfunction and dysfunction diagnosis formulas based on the productive structure of the system. In addition, drawbacks of this method are also exposed. Another diagnosis perspective, driven by characteristic curves, is introduced in Section 3 along with the generic formulas. The case study where both diagnosis methodologies are implemented is defined in Section 4. The application of both methods of diagnosis and the numerical results obtained are covered in Section 5. Finally, the main contributions of the paper and the discussions on the results are summarized in Section 6.

MATRICIAL NOMENCLATURE

- $\mathbf{X}$ (nx1) Generic vector of X variable
- $\mathbf{X_D}$ (nxn) Diagonal matrix of X vector
- $\mathbf{X^0}$ (nx1) Reference condition of generic X vector
- $\Delta\mathbf{X}$ (nx1) Variation of generic X vector between two conditions
- $^{t}\mathbf{X}$ (1xn) Transposed of generic X vector
- $\mathbf{u}$ (nx1) Unitary vector
- $X^{1^{st}}, X^{2^{nd}}$ (1x1) generic value of X for the 1st and 2nd diagnosis calculation

MF & DF ANALISYS

- $\mathbf{P}$ (nx1) Component Product vector
- $\mathbf{P_S}$ (nx1) Final product vector
- $\mathbf{K}$ (nx1) Unit exergy consumption vector
- $\boldsymbol{\kappa_0}$ (nx1) Vector of the marginal exergy consumptions related to the external resources
- $\langle\mathbf{KP}\rangle$ (nxn) Matrix of the marginal exergy consumptions , κ_{ij}
- $|\mathbf{I}\rangle$ (nxn) Matrix irreversibility extended operator
- F_T, F_T^0 (1x1) Resource consumption in real and reference operating conditions
- $\mathbf{MF}$ (nx1) Malfunction vector
- $\mathbf{DF}$ (nx1) Dysfunction vector
- DF_{ij} (−) Components of the Dysfunction matrix

CHARACTERISTIC CURVES

- π (1x1) Generic term for characteristic curves representation
- ξ (1x1) Subset of generic independent variables
- κ (1x1) Specific term for characteristic curves application
- τ (1x1) Subset of specific thermal independent variables
- $\kappa_{i,ind}^{0}$ (1x1) Induced unit exergy consumption of the i^{th} component
- $MF_{i,ind}$ (1x1) Induced malfunction of the i^{th} component
- $MF_{i,int}$ (1x1) Intrinsic malfunction of the i^{th} component

Figure 1: Nomenclature and brief description of symbols grouped according to their purpose

2. THERMOECONOMIC DIAGNOSIS. MF & DF ANALYSIS

General Characteristics

Thermoeconomics relates the thermodynamic parameters with the economic ones based on the idea that *exergy* is the unique parameter which rationally determines the cost of the fluxes; this is due to the fact that exergy takes into account the quality of energy and the irreversible nature of energy conversions [6].

Beyond that, thermoeconomic analysis is based on the *productive structure* [7] of the plant where the interactions between components are identified according to their functional relationships. The exergy flows related to the component resources are labelled as *Fuel*, F, whereas those associated with the desired output are known as *Product*, P, which meanwhile, can be fuel from other components and sometimes from wastes or residues. Components are described by their specific exergy consumptions which refer to the amount of resources needed to produce a unit of product, and this parameter being one of the key variables for diagnosis purposes.

Thermoeconomic diagnosis is difficult to apply in building HVAC systems, precisely because:

- It should be noted that exergy is always evaluated with respect to a reference environment, *dead state*. Exergy methods applied in buildings might seem cumbersome or complex to some people, since not only is a dead state difficult to define but it also changes dynamically over time, and the results might seem difficult to interpret and understand [8].
- The definition of *productive structure* may well lead to controversy [9] due to the dynamic behaviour of thermal installations in buildings. The same system can have more than one productive structure depending upon the switching on and switching off of the components. Likewise, the performance of any component, in fact, is heavily influenced by all other components because of the system

balancing; then, the effects of any anomaly will propagate to the whole plant, due to the complex relationships.

- The most challenging enforcement of thermoeconomic diagnosis is to resolve the *direct problem,* which consists of detecting a possible anomaly and its location. It is a difficult task and the reliability of its results has not yet been proven [10]. For the moment, only the *inverse problem* of diagnosis has been solved, i.e., under the *knowledge* of specific anomalies in different components, the procedure involves quantifying the effects of those anomalies in terms of thermoeconomic quantities, such as fuel impact and malfunctions.

Nevertheless, several thermoeconomic diagnoses have been published during the last years, although most of them are applied to industry. Verda and his co-workers applied a zooming strategy in a combined cycle in order to first locate the macro-component where the anomaly occurs [9], [11]. Besides that, this same author also developed a methodology in which the effects of the control system are filtered [12]. Mendes et al [13] analysed the influence of two different mono-fault cases implemented in a vapour compression refrigeration system, whereas Shi et al [14] discussed the fuel impact that results from malfunctions that occur when two LP heaters are out of service in a 1000 MW supercritical power plant. Piacentino and Talamo [15] proposed an improved thermoeconomic diagnosis method and applied it in a 120 kW air conditioning system and these same authors [16] made a critical analysis on the capabilities and the limits of thermoeconomic diagnosis in a multiple simultaneous faults air-cooled air conditioning system. Finally, it is worth highlighting the study where the effects produced by a mono-fault located on the radiators system of a DHW and heating demand facility is addressed [10].

Malfunction and Dysfunction Analysis

As a brief summary, the diagnosis method is based on the comparison between the real (malfunctioning) and reference (without anomalies) operating conditions. Different indicators can be used to quantify the effects of malfunctions [17]. The additional fuel consumption ΔF_T, or *fuel impact* [18], is the difference between the resource consumption of the plant in operation and in the reference condition:

$$\Delta F_T = F_T - F_T^0 \qquad 1)$$

From that representation, the fuel impact formula can be extended and related to every component as the sum of malfunctions MF_i, dysfunctions DF_i and the final product variation ΔP_{s_i}:

$$\Delta F_T = {}^t\mathbf{u}\cdot[\mathbf{MF} + \mathbf{DF} + \mathbf{\Delta P_S}] \qquad 2)$$

Malfunction in i^{th} component, MF_i, occurs due to an increase of the unit exergy consumption $\Delta\kappa_i$ in the component itself; and DF_i is the variation of the i^{th} component production induced by intrinsic malfunctions in other components. So dysfunctions are not related to a variation of the component efficiency, i.e. they can occur in components whose exergy efficiencies have maintained constant. They are defined as follows [10]:

$$\mathbf{MF} = \mathbf{\Delta K_D}\cdot\mathbf{P^0} \qquad 3)$$

$$\mathbf{DF} = (\mathbf{K_D} - \mathbf{U_D})\cdot\mathbf{\Delta P} \qquad 4)$$

As it will be explained later on, eq(3) and eq(4) can be estimated independently at the component level; this is to say, without considering the relationships between the elements inside the system.

Nevertheless, in addition to this representation, as the distribution of the resources throughout the plant and the interconnections among subsystems are defined by the productive structure, MF and DF analysis can be understood as follows [10]:

$${}^t\mathbf{MF} = {}^t\mathbf{\Delta\kappa_0}\cdot\mathbf{P_D^0} + {}^t\mathbf{u}\cdot\left(\mathbf{\Delta\langle KP\rangle}\cdot\mathbf{P_D^0}\right) \qquad 5)$$

$$\mathbf{DF} = |\mathbf{I}\rangle\cdot\mathbf{\Delta P_s} + \left(|\mathbf{I}\rangle\cdot\mathbf{\Delta\langle KP\rangle}\cdot\mathbf{P_D^0}\right)\cdot\mathbf{u} \qquad 6)$$

were $\Delta\kappa_0$ contains the variation of the marginal exergy consumption associated with the external resources; and $\Delta\langle KP\rangle$ refers to the variation of the marginal exergy consumption of each component (i.e. $\Delta\kappa_{ij}$ accounts the portion of *j* total resources coming from *i* product for the obtainment of a unit of *j* product), whereas $|\mathbf{I}\rangle$ refers to the irreversibility extended matrix operator [19].

In this way, by interpreting the dysfunction matrix **DF**, the induced dysfunction can be related to the malfunction that generates it and to that fostered by $\mathbf{\Delta P_s}$. That is to say, DF_{ij} picks out the dysfunction part of *i* caused by a malfunction in *j* and DF_{i0} reflects the induced consumption variation boosted by the final product variation.

If the reader wants to delve more deeply into diagnosis roots and its mathematical development, the paper [19] together with [10] illustrate the direct way to achieve that aim.

Shortcomings of this method

Although this formula seems very attractive, the contributions given by the malfunction terms should not be confused with the effects due to the *intrinsic malfunctions*, since the variations of unit exergy consumption can be caused by *induced* perturbations as well; or similarly stated, the term $\Delta\kappa_i = \sum_j \Delta\kappa_{ij}$ does not only represent the consumption variation due to an intrinsic anomaly in the i^{th} component but it is also owed to the effects prompted by other components anomalies. Consequently, the contributions given by the terms DF represent only a part of the overall induced effects [17].

Henceforth, induced effects must be detected for a proper study. These effects take place when a component without anomalies works at a non-reference operating condition.

According to [20], malfunctions can be categorized as either internal or external and then distributed in some subcategories. In Figure 2 each type is labelled and shortly explained.

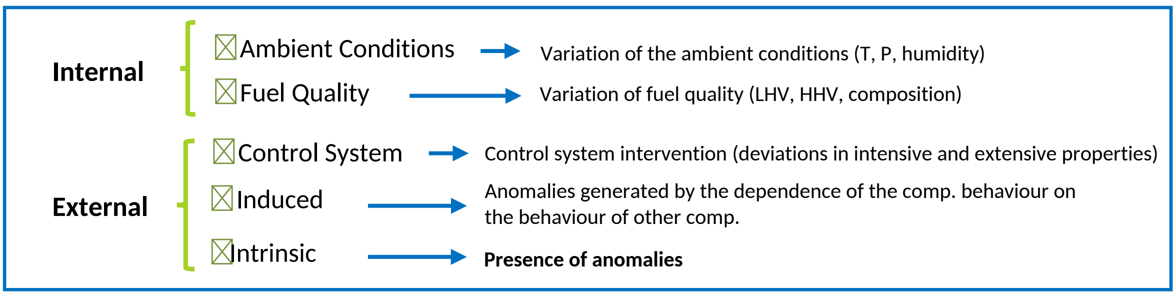

Figure 2: Malfunction Classification

Because different malfunctions take place during a faulty operating condition, and in order to make a reliable diagnosis, the influence of induced effects should be distinguished from the intrinsic ones:

- *External effects* are easily avoided by imposing the same ambient conditions and same fuel quality in both the faulty and reference operating condition.
- *Control system intervention* imposes some barriers to the malfunction propagation which can also be prevented. The effect of an anomaly in a component generally induces a variation in the thermodynamic properties of the downstream flows, but the control system, commanded by some restrictions, acts with the aim of adapting to the new circumstances [12]. This control effect should be filtered to properly compare reference and real faulty operating conditions so that both cases have an equivalent behaviour. An artificial condition is obtained by restoring the same reference regulation condition in the faulty one, known as *free condition*, which should be virtually determined, as is described in [10].
- The main difficulty of this task is the presence of *induced malfunctions*, which appear because unit exergy consumptions are not true independent variables. Some components may present a reduced efficiency, although they are not sources of operating anomalies, due to non-flat efficiency curves. In Lazzaretto and co-workers opinion [17], a rigorous *mathematical* approach based on the true independent variables of the system is therefore required.

As the malfunction and dysfunction analysis does not discriminate between intrinsic and induced malfunctions, it cannot be considered a fully reliable approach. This methodology is effective in the evaluation of the malfunction effects but not in identifying the sources of anomalies.

3. THERMOECONOMIC DIAGNOSIS. CHARACTERISTIC CURVES

General Characteristics

Regarding the objective of searching a rigorous mathematical approach to distinguish induced effects from intrinsic ones, some authors have developed different theories based directly on the thermodynamic description of the model. For instance, Uson and Valero [21] provide a systematic numerical decomposition of malfunctions and malfunction costs into intrinsic and induced effects relying on thermodynamic restrictions of the problem, but unfortunately, it is not a direct procedure. Xu and al. [22], however, based their study on a new indicator proposed by Toffolo and Lazzaretto [23] which accords to the availability of component *characteristic curves* in the reference operating conditions.

The characteristic curves of a i^{th} component consist of a set of relationships expressing a thermodynamic quantity π_i that characterizes the component behaviour as a function of some variables ξ_i involved in the component operation. The generic characteristic curve associated with the reference operating condition takes the form of eq(7) and a specific working point (R) inside that curve is represented by eq(8):

$$\pi_i^0 = f^0\left(\xi_i^0\right) \quad 7)$$

$$\pi_i^{0,R} = f^0\left(\xi_i^{0,R}\right) \quad 8)$$

The selected thermodynamic parameter representing the component π_i can be different depending on the chosen criteria. Toffolo and Lazzaretto [23] recommend component *irreversibility* because then the indicator takes a strictly positive value in case there is a presence of anomalies. Nevertheless, in order to make a direct comparison with the previous diagnosis method, the dependent thermodynamic quantity to express will be the component unit exergy consumption, κ_i. The variables ξ_i chosen for these curves are the mass flow rates, temperatures and pressures, designated as τ_i. Hence, the appearance of the generic characteristic curve used for reference condition eq(9) and its specific working point (R), eq(10), are:

$$\kappa_i^0 = f^0\left(\tau_i^0\right) \qquad 9)$$

$$\kappa_i^{0,R} = f^0\left(\tau_i^{0,R}\right) \qquad 10)$$

Let us now assume that because the induced effects are transferred downstream, the $\tau_i^{0,R}$ values change according to the physical constraints imposed by the component characteristic to $\tau_i^{0,A}$. Therefore, the component will be working in a new operating condition point, A, but still, the point will belong to the reference condition characteristic curve, f^0:

$$\kappa_i^{0,A} = f^0\left(\tau_i^{0,A}\right) \qquad 11)$$

Moreover, let us consider a new situation where the component contains an anomaly, which means the presence of an intrinsic malfunction. In this case again, the component will be in a different working point, B, with different independent variable values, τ_i^B. But nonetheless, since the i^{th} component contains a fault, the characteristic curve connected to faulty condition f would be different from the reference one, f^0:

$$\kappa_i^B = f\left(\tau_i^B\right) \qquad 12)$$

Characteristic Curves Application

This study needs to be individually implemented in each component. As said above, the generic i^{th} component would have two values for its unit exergy consumption, one associated with the reference condition κ_i^0, and the other one with the faulty operating condition κ_i.

According to what was previously explained, even if the component does not contain any anomaly, the independent thermal variables in reference condition $\tau_i^{0,R}$ would be different from those on faulty operating condition τ_i^B, due to induced effects. If the i^{th} component contains a fault, the characteristic curve connected to faulty condition f would be different from reference curve f^0. In that case, a new unit exergy consumption value can be calculated eq(13); this is mathematically obtained by inserting the values of the independent variables of faulty operating conditions in the reference characteristic curve.

$$\kappa_{i,ind}^{0} = f^0\left(\tau_i^{o,A}\right) \quad 13)$$

Figure 3 depicts the three cases.

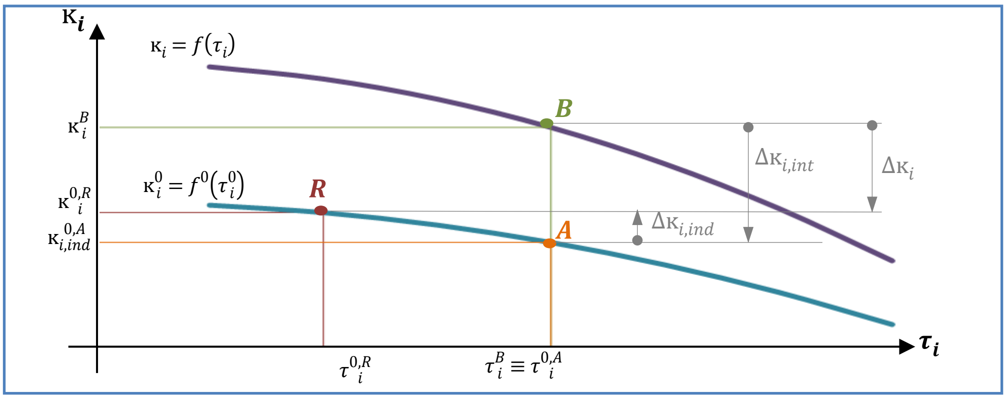

Figure 3: Unit exergy consumption in reference and operating

As a result, the increase of the unit exergy consumption, $\Delta\kappa_i$, can be divided into induced and intrinsic unit exergy consumption variation, $\Delta\kappa_{i,ind}$, $\Delta\kappa_{i,int}$, as follows:

$$\Delta\kappa_{i,ind} = \kappa_{i,}^0\left(\tau_i^A\right) - \kappa_i^0\left(\tau_i^R\right) \quad 14)$$
$$\Delta\kappa_{i,int} = \kappa_i\left(\tau_i^B\right) - \kappa_i^0\left(\tau_i^A\right) \quad 15)$$

Consequently, according to eq(3) the malfunction of each component can be expressed as the sum of intrinsic and induced malfunctions:

$$MF_i = MF_{i,int} + MF_{i,ind} = \Delta\kappa_{i,int} \cdot P_i^0 + \Delta\kappa_{i,ind} \cdot P_i^0 \quad 16)$$

This formulation allows calculating individually the effects that anomalies produce in every component depending on the thermodynamic independent variables.

A generic procedure is therefore established to locate the origin of system intrinsic and induced malfunctions from the analysis of the faulty operating conditions, where the only possible source of uncertainty is the inaccuracy in the reconstruction of component characteristic curves, due to the required amount of data.

Revision of both Methodologies

Both techniques of thermoeconomic diagnosis give different essential information:

- Malfunction and dysfunction diagnosis procedure uses the Fuel-Product productive structure in order to relate each component inputs and outputs to the rest of the subsystems. It does not differentiate between intrinsic and induced malfunction but, the dysfunctions provoked by j belonging to a malfunction in i can be estimated, as well as those generated due to the final production variations. Likewise, the way that the whole plant efficiency changes when the efficiency of any component varies can also be easily calculated. Moreover, as the productive structure is also used for cost accounting, either the *exergetic cost* or the *economic cost* of every flow and of the overall system can be assessed as well [19], in addition to the *cost impact* generated by the anomalies [10].
- Characteristic curves change the perspective and refer to the components individually. This method enables researchers to distinguish between the induced and intrinsic malfunctions in every component by considering the actual links among the thermodynamic variables (pressure, temperature mass flows and composition) and the exergy unitary consumptions.

Combination of both methodologies . Fault detection approach

Supposing that *more than one* intrinsic malfunction has taken place in the system, the MF and DF diagnosis is not able to furnish any information about the incidence of each one on the total fuel impact, since the irreversibility variation causes a different fuel impact depending on the position of the component where the fault has occurred.

When various anomalies appear in the system, each anomaly would induce effects in the j^{th} component with the anomaly itself, varying its $\Delta\kappa_{j,int}$ (intrinsic malfunction) and in the rest of i^{th} components varying both the unit exergy consumption, $\Delta\kappa_{i,ind}$ (induced malfunctions), and the local production, ΔP_i (dysfunctions). The objective is to distinguish between the $\Delta\kappa_{i,ind}$ and ΔP_i produced by each anomaly so the extra consumption can be attributed to the j^{th} malfunctioning component which has generated them. Thanks to the MF and DF diagnosis, this last extra consumption provoked by j related to the ΔP_i variation is accounted for through DF_{ij}, but further information is needed for accounting the remaining induced malfunction effects.

Consequently, if the information acquired by this diagnosis is complemented with the characteristic curves analysis, the subsystem with higher intrinsic malfunction can be recognized and identified as the faultiest component. However, even now, the extra consumption caused by $\Delta\kappa_{i,ind}$ cannot be attributed to any component, nor can the one belonging to the final production variation ΔP_s, because this analysis is individually performed and the induced effects could have been caused by more than one different component.

Notwithstanding these barriers, thanks to characteristic curves analysis, the component identified as the faultiest one (let's say j component) can be virtually erased and a second diagnosis study can be executed. In this way, the decrease of the fuel impact accounted from the first study, $\Delta \mathrm{F}^{1^{st}}_T$, to the next one , $\Delta \mathrm{F}^{2^{nd}}_T$, would express the savings gained when the anomaly in j is repaired:

$$\Delta F_{save} = \Delta \mathrm{F}^{1^{st}}_T - \Delta \mathrm{F}^{2^{nd}}_T \qquad 17)$$

In the same way, that ΔF_{save} would correspond to the sum of the intrinsic malfunctions in j $\left(MF^{1^{st}}_{j,int}\right)$ and its induced effects calculated in the first study $\left(\sum_i DF^{1^{st}}_{ij} + \sum_i MF^{1^{st}}_{ij,ind}\right)$ plus the final production variation $\left(\Delta\Delta P^{1^{st},2^{\mathrm{nd}}}_s\right)$ and the dysfunction it generates between both situations $\left(\Delta DF^{1^{st},2^{\mathrm{nd}}}_0\right)$:

$$\Delta F_{save} = \left[MF^{1^{st}}_{j,int} + \sum_i DF^{1^{st}}_{ij} + \sum_i MF^{1^{st}}_{ij,ind}\right] + \left[\left(DF^{1^{st}}_o - DF^{2^{nd}}_0\right) + \left(\Delta P^{1^{st}}_s - \Delta P^{2^{nd}}_s\right)\right] \qquad 18)$$

As $MF^{1^{st}}_{j,int}$, $\Sigma_i DF^{1^{st}}_{ij}$ and $DF^{1^{st},2^{nd}}_{0}$, $\Delta P^{1^{st},2^{nd}}_{s}$ are calculated through one of the above methodologies, $\Sigma_i MF^{1^{st}}_{ij,ind}$ can be easily obtained with a simple subtraction.

If this is repeated as many times, or steps, as intrinsic malfunctions exist, the diagnosis inverse problem is solved. Figure 4 outlines the methodology routine.

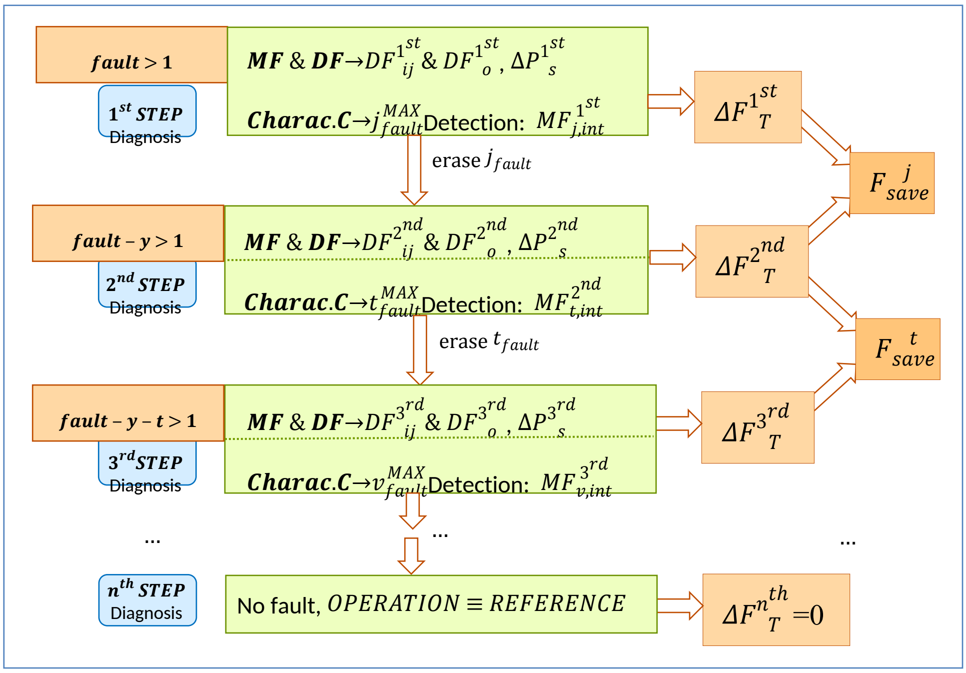

Figure 4: Diagnosis methodology through the combination of MF&DF study and characteristic curves

4. DYNAMIC CASE STUDY

Preliminary work

The two diagnosis methods presented above will be applied in a heating and DHW plant in order to highlight its characteristics, compare both methodologies and complement them in a *dynamic building environment.* Let's assume there is a *multi-fault* case where some anomalies are intentionally introduced.

First of all, it is recommended to highlight that research on building thermal facilities implies *dynamic studies* according to the changing behaviour of the variables such as climate, user demand and so on, which directly interferes in the start-up and shutdowns of the elements integrated in the installation. On the other hand, as diagnosis involves the *comparison* between two operating conditions, dynamic simulation of the faulty (with anomalies) and the reference conditions needs to be done, while in both the heating and the DHW demand should be kept the same.

As previously stated, the ambient conditions during the heating season coincide in both simulations, as well as the fuel quality and composition; the control system intervention effect is avoided through the free condition obtainment which is fully explained in [10]. Because of the free condition achievement and due to the arguments displayed in [10], a DHW production output variation would inevitably exist $\Delta P_{s_{DHW}} \neq 0$, being indeed $\Delta P_{s_{DHW}} < 0$.

The simulation is done with a 30s time-step and the reference operating condition data and free condition data (named as faulty condition) is extracted every *hour* during the heating season. So the dynamic study is represented as a set of hourly quasi-static states joined by one after the other.

General description of the facility

The reference generic facility coincides with the one used in [10], where a full explanation of all components can be found; additionally, in this case, the pumps are considered in the study. The system covers the heating and DHW demand of a 16 householder multi-family flat located in Bilbao (Spain), through a typical heating installation in the Basque Country [24].

As a general explanation, the energy supply system consists of a 28 kW natural gas boiler. Other components are a 35 litter hydraulic compensator, three way valves, a heat exchanger and a 1000 litter DHW storage tank, see Figure 5; the heating demand is represented through the heat dissipation of a radiator system and a 3-way valve. The DHW is given by a DHW tank and a 3-way valve that ensures hot water at a constant temperature.

As extensively explained in [26], before any calculation a decision must be made with respect to whether the analysis of the components should be conducted using total exergy or separate forms of it (i.e. thermal, mechanical and chemical exergies). Even if splitting the exergy refines the accuracy, the computational efforts are much higher than the obtained improvements; the corrections are often marginal and they are not necessary for extracting the main conclusions from the exergoeconomic diagnosis evaluation. For that reason, the total exergy will be considered in the research.

Overall a total of 13 components were listed and described in Table 1, and 28 flows were considered for the study, as seen in Figure 5. Different inputs coming from three external

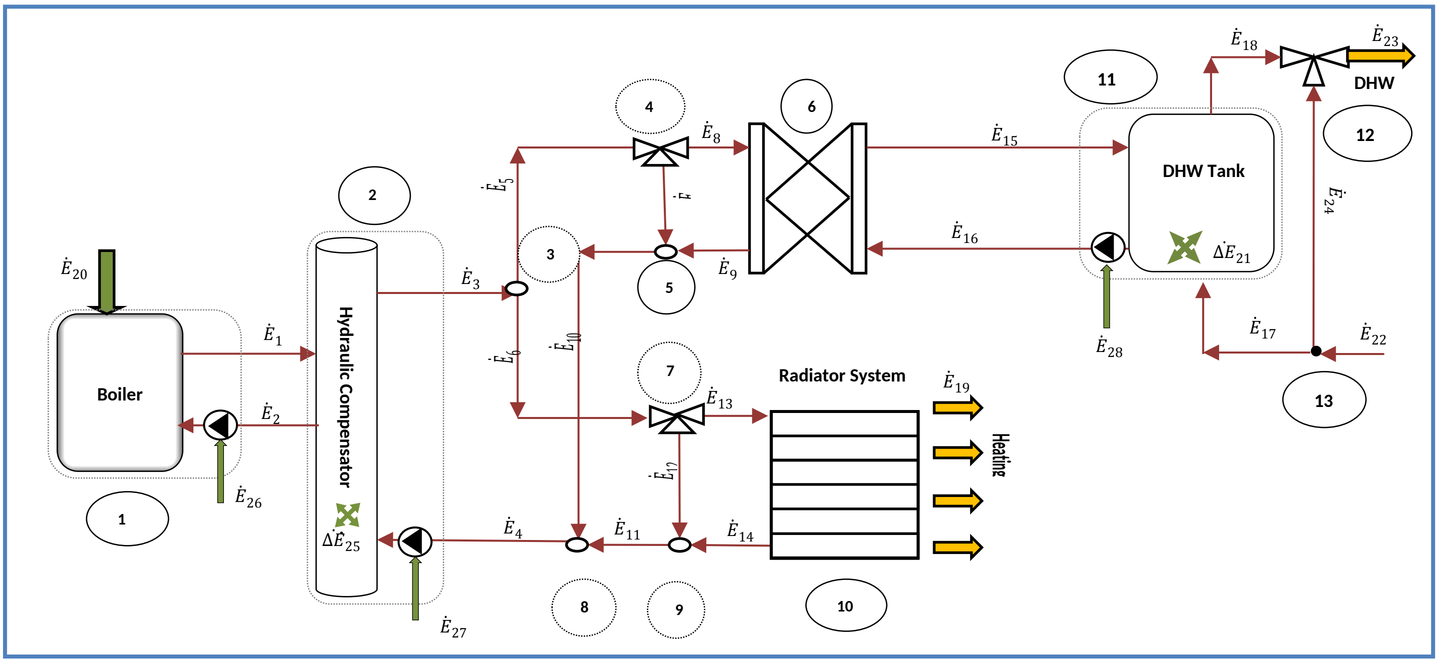

Figure 5: Physical Structure of the facility

sources are noted: (1) natural gas ($\dot{E}_{20}$), (2) the contribution given by the hydraulic compensator ($\Delta\dot{E}_{25}$) and the tank ($\Delta\dot{E}_{21}$), which are the difference between the initial and final exergy those components have in the considered period, and (3) three inputs coming from the electrical grid, one for powering each pump ($\dot{E}_{26}$,$\dot{E}_{27}$, $\dot{E}_{28}$). Those are represented by green arrows whereas yellow arrows indicate the final products leaving the system, such as DHW ($\dot{E}_{23}$) and heating demand ($\dot{E}_{19}$).

The various components appearing in the case study are simulated using simplified models available from the Trnsys v17 library. The *control* that turns on and deactivates the devices of the plant is insightfully detailed in [10].

Thermoeconomic Diagnosis

As mentioned, the dynamic simulation will provide the hourly data required for the calculation of every exergy flow $\dot{E}_i$ eq(20). Then, a thermodynamic diagnosis will be completed hourly by eq(5) and eq(6) and afterwards, the malfunctions and dysfunctions accumulated at the end of the studied period will be calculated. Consequently, the fuel impact according to the incorporation of those anomalies is also quantified.

The first and probably the most sensitive step for this analysis is defining the productive structure for each time-step following the pattern given in [19]. As previously remarked, the system dynamic behaviour interferes in the start-up and shutdowns of the components, so that the productive structure varies depending on the components which are turned on in that precise moment. Figure 6 illustrates two of the possible cases: case 1 depicts the situation where only DHW demand is requested; case 2 shows the situation where only heating demand is claimed. Both cases are associated with two different productive structures.

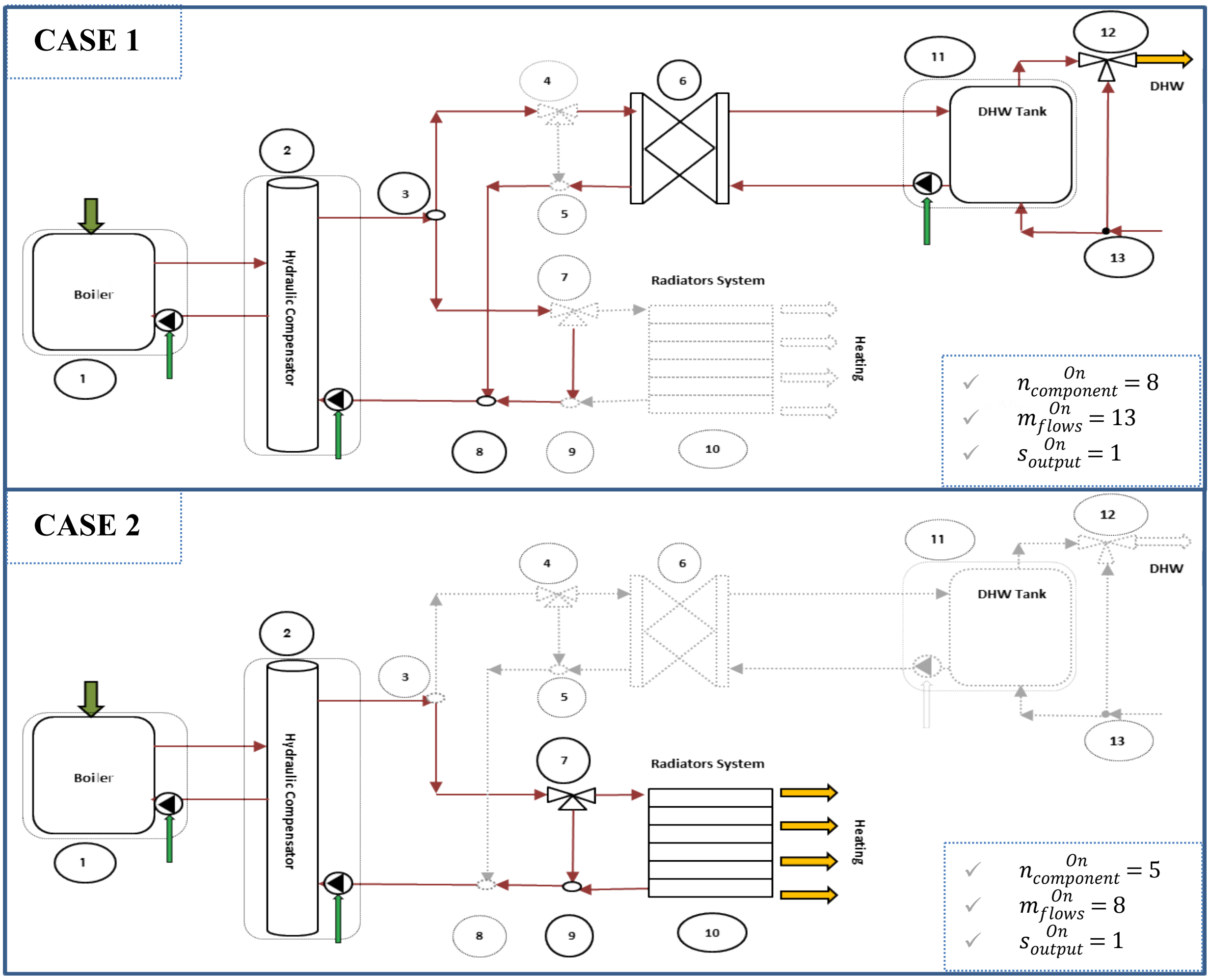

Figure 6: Different operation situations related to different productive structures

Although all the components do not have to be simultaneously switched on, Table 1 specifies F, P and κ for every component according to the nomenclature in Figure 5.

Table 1: F/P Table and exergy unitary consumption of each subsystem

n	COMPONENT		F_i	P_i	κ_i
①	Cond. Boiler + Gen. Pump	CB	$\dot{E}_{20}$	$\dot{E}_1 - \dot{E}_2$	$\dot{E}_{20}/(\dot{E}_1 - \dot{E}_2)$
②	Compensator + Dist. Pump	HC	$(\dot{E}_1 - \dot{E}_2) + \Delta\dot{E}_{25}$	$\dot{E}_3 - \dot{E}_4$	$[(\dot{E}_1 - \dot{E}_2) + \Delta\dot{E}_{25}]/(\dot{E}_3 - \dot{E}_4)$
③	Heating & DHW Diverter	D1	$\dot{E}_3$	$\dot{E}_5 + \dot{E}_6$	$\dot{E}_3/(\dot{E}_5 + \dot{E}_6)$
④	DHW 3-way valve	V1	$\dot{E}_5$	$\dot{E}_7 + \dot{E}_8$	$\dot{E}_5/(\dot{E}_7 + \dot{E}_8)$
⑤	DHW Mixer	M1	$\dot{E}_7 + \dot{E}_9$	$\dot{E}_{10}$	$(\dot{E}_7 + \dot{E}_9)/\dot{E}_{10}$
⑥	Heat Exchanger	HX	$\dot{E}_8 - \dot{E}_9$	$\dot{E}_{15} - \dot{E}_{16}$	$(\dot{E}_8 - \dot{E}_9)/(\dot{E}_{15} - \dot{E}_{16})$
⑦	Heating 3-way valve	V2	$\dot{E}_6$	$\dot{E}_{12} + \dot{E}_{13}$	$\dot{E}_6/(\dot{E}_{12} + \dot{E}_{13})$
⑧	Heating & DHW Mixer	M2	$\dot{E}_{10} + \dot{E}_{11}$	$\dot{E}_8$	$(\dot{E}_{10} + \dot{E}_{11})/\dot{E}_8$
⑨	Heating Mixer	M3	$\dot{E}_{12} + \dot{E}_{14}$	$\dot{E}_{11}$	$(\dot{E}_{12} + \dot{E}_{14})/\dot{E}_8$
⑩	Radiators System	RS	$\dot{E}_{13} - \dot{E}_{14}$	$\dot{E}_{19}$	$(\dot{E}_{13} - \dot{E}_{14})/\dot{E}_{19}$
⑪	DHW Tank + Storg. Pump	T	$(\dot{E}_{15} - \dot{E}_{16}) + \Delta\dot{E}_{21}$	$\dot{E}_{18} - \dot{E}_{17}$	$[(\dot{E}_{15} - \dot{E}_{16}) + \Delta\dot{E}_{21}]/(\dot{E}_{18} - \dot{E}_{17})$
⑫	DHW 3-way valve	V3	$\dot{E}_{18} + \dot{E}_{24}$	$\dot{E}_{23}$	$(\dot{E}_{18} + \dot{E}_{24})/\dot{E}_{23}$
⑬	DHW Diverter	D2	$\dot{E}_{22}$	$\dot{E}_{17} + \dot{E}_{24}$	$\dot{E}_{22}/(\dot{E}_{17} + \dot{E}_{24})$

Characteristic curves Diagnosis

As previously pointed out, building facilities are strictly linked to dynamic fluctuations. At every time-step the thermodynamic variables τ change so the unit exergy consumption κ of every component also varies. This means that, in the same way as for the earlier method, the study should be repeated for each component individually for every hour during the whole heating season. Afterwards, as in the previous diagnosis, the cumulative values of malfunctions and dysfunctions drawn through this representation will be accounted for using eq(3) and eq(4).

As there are 13 components, at least 13 characteristic curves must be defined. The main goal is to define a curve which recreates the same component behaviour as the one in the previous diagnosis, which is based on the Trnsys v17 algorithm. For that purpose, the Trnsys component mathematical reference guidebook [25] together with its Fortran programming have been analysed. In such way, the independent variables τ_i and physical specific characteristics of every component have been considered. As an example, here there is an explanation as to how to calculate the heat exchanger characteristic curve:

One needs to bear in mind the definition of its unit exergy consumption, which is written in Table 1:

$$\kappa_6 = \frac{\dot{E}_8 - \dot{E}_9}{\dot{E}_{15} - \dot{E}_{16}} \qquad 19)$$

The formula for the generic physical i water exergy flow is expressed as follows:

$$\dot{E}_i = c_P \cdot \dot{m} \cdot T_i - T_0 - T_0 \cdot ln\left(\frac{T_i}{T_0}\right) \qquad 20)$$

were c_p is the fluid specific heat, $\dot{m}$ is the mass flow rate and T_0 refers to the ambient temperature.

The independent variables τ_6 and physical characteristics chosen for the heat exchanger are the primary and secondary inlet temperatures (T_8,T_{16}) (which are likewise outputs of V1 and T), the mass flow rates ($\dot{m}_{prim}$,$\dot{m}_{sec}$), the ambient temperature (T_0) and the overall heat transfer coefficient UA. So that (T_9,T_{15}) output temperatures depend on those variables.

In order to calculate them, the Trnsys heat exchanger algorithm relies on the effectiveness approach: the model starts determining whether the primary or the secondary side is the minimum capacitance side:

$$C_{prim} = c_P \cdot \dot{m}_{prim} \qquad 21)$$
$$C_{sec} = c_P \cdot \dot{m}_{sec} \qquad 22)$$
$$C_{max} = \max\left(C_{prim}, C_{sec}\right) \qquad 23)$$
$$C_{min} = \min\left(C_{prim}, C_{sec}\right) \qquad 24)$$

After that, it calculates the effectiveness based upon the specified flow configuration and on UA:

$$\varepsilon = \frac{1 - e^{\left(-\frac{UA}{C_{min}} \cdot \left(1 - \frac{C_{min}}{C_{max}}\right)\right)}}{1 - \frac{C_{min}}{C_{max}} \cdot e^{\left(-\frac{UA}{C_{min}} \cdot \left(1 - \frac{C_{min}}{C_{max}}\right)\right)}} \qquad 25)$$

Following this trajectory, the heat exchanger outlet temperatures are computed, which would be at the same time the input parameters of M1 and T.

$$T_9 = T_8 - \varepsilon \cdot \left(\frac{C_{min}}{C_{prim}}\right) \cdot (T_8 - T_{16}) \quad 26)$$

$$T_{15} = T_{16} + \varepsilon \cdot \left(\frac{C_{min}}{C_{sec}}\right) \cdot (T_8 - T_{16}) \quad 27)$$

In this way κ_6 can be calculated and plotted. Figure 7 depicts the behaviour of κ_6 when one of its independent variables changes its value while the others remain constant.

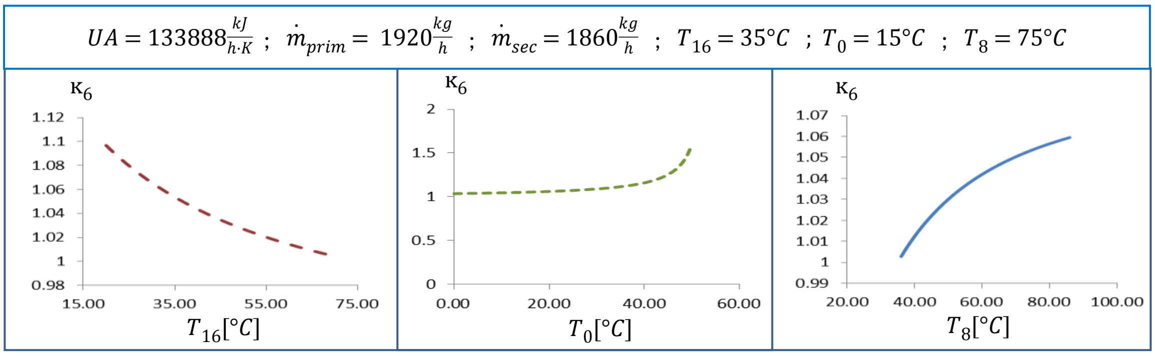

Figure 7: Heat exchanger characteristic curves related to the fluctuation of one independent variable

5. NUMERICAL EXAMPLE

The DHW and space heating energy demand are calculated in the same way as in [9] both accounting for the whole heating season comprising from the 1st of November until the 30th of April.

Multi-Faults

As any component can be chosen for containing the fault and the effects that it would produce depending on the location of that component, two faults are deliberately incorporated on the *radiator system* and *heat exchanger* by degrading some of their physical characteristics. An anomaly is set through a 10% reduction in the RS *energy performance*; and in HX the *overall heat transfer coefficient* is diminished 35%. The reference and operation condition simulation are independently undertaken.

Figure 8 depicts the reference and faulty operation characteristic curves of those components when one of their independent variables changes its value while the rest remain constant.

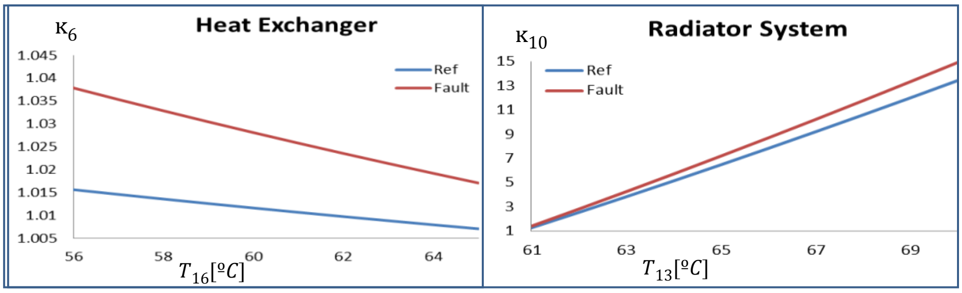

Figure 8: Characteristic curves of reference and faulty components

Simulation and a calculation of the exergy flows are performed hourly. For their calculation, hourly ambient conditions are taken as *dead state* so, dynamic values are regarded. Table 2 is afterwards built, where the accumulated exergy of every flow at the end of the simulation period for reference and faulty operating conditions can be seen.

Table 2: Accumulated exergy values for reference and faulty operating condition $[GJ_{ex}]$

$[GJ]$	E_1	E_2	E_3	E_4	E_5	E_6	E_7	E_8	E_9	E_{10}	E_{11}	E_{12}	E_{13}	E_{14}
$Ref.$	122.9	100.1	372.3	351.8	192.0	180.3	153.3	38.9	29.8	182.9	169.2	57.6	122.7	111.6
$Fault$	122.9	99.2	369.8	348.4	190.7	179.1	151.9	38.8	29.8	181.7	166.7	57.7	121.4	109.2

E_{15}	E_{16}	E_{17}	E_{18}	E_{19}	E_{20}	ΔE_{21}	E_{22}	E_{23}	E_{24}	ΔE_{25}	E_{26}	E_{27}	E_{28}
37.2	28.3	0.2	6.5	2.3	149.1	0.04	0.2	5.8	0.03	0.0	1.7	5.9	0.5
36.2	27.5	0.2	6.4	2.3	155.3	0.05	0.2	5.6	0.03	0.0	1.7	5.9	0.5

Thermoeconomic Diagnosis

At first, an hourly MF and DF diagnosis with two faults is carried out and the values obtained are accumulated later on, see Table 3. The first column identifies each component with its corresponding number. The second column contains the malfunction, MF_i, of every component, eq(5). The expanded dysfunction matrix comes next where the dysfunction according to the exergy consumption variation associated with the external resources, DF_0, and the other components, DF_{ij}, are reflected, eq(6). The last column corresponds to the final product variation, according to eq(2).

Table 3: MF and DF tables extracted from diagnosis accumulation $[MJ]$

	MF & *DF* 1^{st} DIAGNOSIS															
	$MF^{1^{st}}$	$DF^{1^{st}}_0$	$[DF^{1^{st}}]$													$\Delta P^{1^{st}}_s$
		⓪	①	②	③	④	⑤	⑥	⑦	⑧	⑨	⑩	⑪	⑫	⑬	
①	-1214	-1396	-	557	-24	-	-	1255	-	-486	-	6617	-34	-21	-	-
②	-450	-9	-	-	-80	-	-	-48	-	52	-	480	104	-	-	-
③	-	-	-	-	-	-	-	-	-	-	-	-	-	-	-	-
④	-	-	-	-	-	-	-	-	-	-	-	-	-	-	-	-
⑤	-	-	-	-	-	-	-	-	-	-	-	-	-	-	-	-
⑥	206	-12	-	-	-	-	-	-	-	-	-	-	-10	-	-	-
⑦	-	-	-	-	-	-	-	-	-	-	-	-	-	-	-	-
⑧	-136	-14	-	-	87	-	-	32	-	-23	-	-15	-25	-	-	-
⑨	-	-	-	-	-	-	-	-	-	-	-	-	-	-	-	-
⑩	1093	-	-	-	-	-	-	-	-	-	-	-	-	-	-	-
⑪	-40	-6	-	-	-	-	-	-	-	-	-	-	-	-	-	-
⑫	-1	-15	-	-	-	-	-	-	-	-	-	-	-	-	-	-129
⑬	-	-	-	-	-	-	-	-	-	-	-	-	-	-	-	-

- As was predicted, the components with higher malfunctions are those containing the anomalies (components HX, and RS; $MF^{1^{st}}_6 = 206\ MJ$ and $MF^{1^{st}}_{10} = 1093\ MJ$ repectively). However, these values are related to both intrinsic and induced malfunctions so *no immediate conclusions* can be extracted.
- This is also the reason why the other components exhibit non null values for the malfunctions ($MF^{1^{st}}_1 =- 1214\ MJ$; $MF^{1^{st}}_2 =- 450\ MJ$; $MF^{1^{st}}_8 =- 136\ MJ$; $MF^{1^{st}}_{11} =- 40\ MJ$ and $MF^{1^{st}}_{12} =- 1\ MJ$) due to the propagation of induced effects throughout the system which generates a $\Delta\kappa_i < 0$.
- As justified in [10], since the free condition is imposed, the faults produce less final product variation, $\Delta P^{1^{st}}_s < 0$. This fact influences each component's performance inducing a negative $\sum_i DF^{1^{st}}_{i,0} =- 1452\ MJ$.
- Mostly all malfunctions generate a local output variation; therefore, a dysfunction is created. The $DF^{1^{st}}_{i,j}$ matrix element exhibits the dysfunction part of ?? caused by a

malfunction in ??. The effects are commonly suffered by the components located upstream of the anomalies. Consequently, CB is the one undergoing the highest dysfunctions (sum of the 1st line): $DF_{1}^{1^{st}} = DF_{1,2}^{1^{st}} + DF_{1,3}^{1^{st}} + DF_{1,6}^{1^{st}} + DF_{1,10}^{1^{st}} + DF_{1,11}^{1^{st}} + DF_{1,12}^{1^{st}} = 7864\ MJ$.

- Conversely, RS is the component inducing the greatest dysfunction (sum of the 10th column): $DF_{1,10}^{1^{st}} + DF_{2,10}^{1^{st}} + DF_{6,10}^{1^{st}} + DF_{8,10}^{1^{st}} = 7082\ MJ$.
- The dysfunctions generated by HX $\left(\sum_i DF_{i,6}^{1^{st}} = 1239\ MJ\right)$ are also noticeable, but do not cause as much impact because they are located ahead in the supply chain.
- The existence of $\Delta P_{s_{DHW}}^{1^{st}} < 0$ is reflected in the last column.
- The sum of all components, according to eq(2), reflects the fuel impact related to the first diagnosis with three anomalies: $\Delta F_{T}^{1^{st}} = 6296\ MJ$.

Characteristic curves Diagnosis

Alternative analysis has been done considering the characteristic curves diagnosis methodology and has been applied hourly in every component. Subsequently, the values achieved as a result of the first analysis step are accumulated and depicted in Table 4. The column entitled as $\mathrm{MF}_{\mathrm{int}}^{1^{st}}$ contains the intrinsic malfunctions derived from anomalies, eq(16); the column $\mathrm{MF}_{\mathrm{ind}}^{1^{st}}$, alternatively , displays the induced malfunction due to the non-

Table 4: MF and DF first analysis step through characteristic curves

		CHARACTERISTIC CURVES		
		$\mathrm{MF}_{\mathrm{int}}^{1^{st}}$	$\mathrm{MF}_{\mathrm{ind}}^{1^{st}}$	$\mathrm{DF}^{1^{st}}$
①	CB	-	-1214	6467
②	HC	-	-450	500
③	D1	-	-	-
④	V1	-	-	-
⑤	M1	-	-	-
⑥	HX	323	-117	-22
⑦	V2	-	-	-
⑧	M2	-	-136	42
⑨	M3	-	-	-
⑩	RS	1212	-119	-
⑪	T	-	-40	-6
⑫	V3	-	-1	-15
⑬	D2	-	-	-

flat efficiency curves, eq(15). The sum of both columns indicates the total malfunction for each component. The last column remarks the dysfunction values obtained by eq(5).

- This procedure allows dividing and quantifying the induced malfunctions from the intrinsic ones. Henceforth, the results show clearly that the components with intrinsic malfunctions are $\left(MF^{1^{st}}_{6,int} = 323\ MJ\right)$ and $\left(MF^{1^{st}}_{10,int} = 1212\ MJ\right)$; therefore the components are HX and RS respectively.
- Nevertheless, this methodology does not permit one to identify the source of every component dysfunction, but only to calculate the total dysfunction $DF^{1^{st}}_{i}$ value.

Combination of both methods

As more than one intrinsic malfunction has taken place in the system, the subsystem with higher intrinsic malfunction can be recognized and identified as the faultiest component, in this case the RS. After erasing that anomaly, that is, restoring its reference energy performance, another simulation has been conducted in order to quantify the decrease of fuel impact accounted from the first study to the second one. In order to save space, the MF results of characteristic curves of the second analysis step are shown in Table 5,

Table 5: MF, DF and ΔPs analysis in the second analysis step

	CHARACTERISTIC CURVES		**MF & *DF* DIAGNOSIS**		
	$MF^{2^{nd}}_{int}$	$MF^{2^{nd}}_{ind}$	$DF^{2^{nd}}_{0}$	$DF^{2^{nd}}$	$\Delta P^{2^{nd}}_{s}$
① CB	-	-2048	-754	2197	-
② HC	-	-143	1	82	-
③ D1	-	-	-	-	-
④ V1	-	-	-	-	-
⑤ M1	-	-	-	-	-
⑥ HX	317	-118	-6	-9	-
⑦ V2	-	-	-	-	-
⑧ M2	-	-45	-11	59	-
⑨ M3	-	-	-	-	-
⑩ RS	-	18	-	-	-
⑪ T	-	-33	-12	-	-
⑫ V3	-	-1	-10	-	-76
⑬ D2	-	-	-	-	-

together with the DF, DF_0 and the final product vector taken from the other diagnosis analysis.

- In this 2^{nd} case, as the anomaly in RS is corrected, only HX has intrinsic malfunctions, where $\left(MF_{6,int}^{2^{nd}} = 317\ MJ\right)$ outstands among all. Its value is slightly different to the one in the first study, owing to the reparation of the faultiest component that varies the faulty thermodynamic operation conditions.
- $DF_{i,0}^{2^{nd}}$ is again very remarkable. Indeed, as the fault is on the HX, the DHW final production is still lower than in the reference condition and that has an influence on the consumption reduction $\left(\sum_i DF_{i,0}^{2^{nd}} = -792\ MJ\right)$.
- In this case, as fewer anomalies are taken into account, $\Delta P_{s_{DHW}}^{2^{nd}}$ is closer to zero.
- The fuel impact related to the second diagnosis with one anomaly is: $\Delta F_{T}^{2^{nd}} = -590\ MJ$.

Therefore, it is in accordance with eq(17): $\Delta F_{save} = 6886\ MJ$.

So that, regarding eq(18), the induced malfunction generated by the anomaly in RS is equal to: $\sum_{10} MF_{10j,ind}^{1^{st}} = -695\ MJ$.

General results are summarized in Table 6 where each column corresponds to one of the anomalies deliberately inserted in the study and the rows MF_{int}, $\sum MF_{ind}$ and $\sum DF$ correspond to the intrinsic, induced malfunctions and dysfunctions the faulty components have in every study; the row $DF_0+\Delta P_s$ indicates the effect the anomaly produces in the final production variation and its consequences. Finally, the $\Delta F_{anomaly}$ outlines the fuel impact of each anomaly.

Table 6: Diagnosis general results [MJ]

	RS' $anomaly$	HX' $anomaly$
MF_{int}	1212	317
$\sum MF_{ind}$	-695	-1270
$\sum DF$	7082	1230
$DF_0 + \Delta P_s$	-714	-867
$\Delta F_{anomaly}$	6886	-590

In this way the weight of fuel impact on each anomalous component can be attributed:

- The fault in RS generates an extra consumption of 6886 MJ where 7599 MJ are due to the fault itself and the remaining -714 MJ are owed to the final production decrease.
- The fault in HX generates an extra consumption of -590 MJ where 277 MJ are due to the fault itself and the remaining -867 MJ are owed to the final production decrease.

6. CONCLUSIONS AND DISCUSSION

The principle goal of the thermodynamic diagnosis of a system is the detection of the arising anomalies, the identification of the causes and the quantification of the effects.

Although diagnosis allows foreseeing possible breakdowns or preventing energy and economical extra charges, it has seldom been applied in *building thermal facilities*.

The main challenge of applying diagnoses to building thermal facilities is due to the need of the *dynamic representation* of the system. To do such type of analysis, hourly quasi-static states are joined together in order to typify the variable behaviour.

Henceforth, the productive structure of the system varies according to the component activation and deactivation. Besides the structure modifications, the independent variables of every component also change, so κ_i varies in each time-step as well. Therefore, the diagnosis methodologies should be calculated hourly and then the values obtained must be gathered until the end of the study period.

The *malfunction and dysfunction method* has been proved to be effective in evaluating malfunction effects, but appears to be ineffective in associating the extra consumption of the components with anomalies. In the case analysed in this paper, we conclude that it is not possible to signal the component where the intrinsic anomaly is present without a mathematical approach that separates it between intrinsic and malfunction analysis.

Conversely *characteristic curves* diagnosis methodology allows one to account for each component's *intrinsic* and *induced* malfunction on an individual basis.

While conventional diagnosis is achieved through the whole system *productive structure*, characteristic curves analysis is performed in each component individually.

The key finding is that neither of the methodologies is better than the other but they are complementary for a proper diagnosis. By means of the malfunction and dysfunction method, the fuel impact due to each malfunction can be accounted for and the one owing to the final production variation can be identified. Nonetheless, the method does not allow distinguishing between intrinsic and induced effects. On the contrary, the individual characteristic curves methodology allows us to differentiate them. By combining both theories, the fuel impact associated with each anomaly can be calculated through a reiterative diagnosis study.

Hence, the methodology allows studying components in a local way and learning how they affect globally. Hence, not only the efficiency degradation of the abnormal components are detected but also is accounted the extra fuel charge generated by each fault.

This theory is applied in a DHW and heating facility with two faults where RS is identified as the faultiest component. It provokes an overall extra consumption of $6886\ MJ$ during the heating period because of the incited effects on the others ($6387\ MJ$), the effects prompted in the component itself ($1212\ MJ$) and that are generated by changing the final production ($-714\ MJ$).

Acknowledments

The author, A Picallo, acknowledges the support provided to her by the Ministry of Education of the Spanish Government through a scholarship granted to her to complete her PhD degree. The authors also acknowledge the support provided by the Laboratory for the Quality Control in Buildings of the Basque Government.

REFERENCES

[1] Pérez-Lombard, L., Ortiz, J., & Pout, C. (2008). A review on buildings energy consumption information. Energy and Buildings, 40(3), 394-398.

[2] Piacentino, A., & Catrini, P. (2016). Assessing the Robustness of Thermoeconomic Diagnosis of Fouled Evaporators: Sensitivity Analysis of the Exergetic Performance of Direct Expansion Coils. Entropy, 18(3), 85

[3] Lozano, M. A., Bartolomé, J. L., Valero, A., & Reini, M. (1994). Thermoeconomic diagnosis of energy systems. In Flowers (Vol. 94, pp. 149-156).

[4] Torres, C., Valero, A., Serra, L., & Royo, J. (2002). Structural theory and thermoeconomic diagnosis: Part I. On malfunction and dysfunction analysis. Energy Conversion and Management, 43(9), 1503-1518.

[5] Toffolo, A., & Lazzaretto, A. (2007). A new thermoeconomic method for the location of causes of malfunctions in energy systems. Journal of Energy Resources Technology, 129(1), 1-9.

[6] Sciubba, E. (2001). Beyond thermoeconomics. The concept of extended exergy accounting and its application to the analysis and design of thermal systems. Exergy, an international journal, 1(2), 68-84.

[7] Torres, C., et al. (1996) The productive structure and thermoeconomic theories of system optimization. American Society of Mechanical Engineers, New York, NY (United States).

[8] Hepbasli, A. (2012). Low exergy (LowEx) heating and cooling systems for sustainable buildings and societies. Renewable and Sustainable Energy Reviews, 16(1), 73-104.

[9] Verda, V., Serra, L., & Valero, A. (2002). Thermoeconomic Diagnosis: Zooming Strategy Applied to Highly Complex Energy Systems—Part 2: On the Choice of the Productive Structure. In ASME 2002 International Mechanical Engineering Congress and Exposition (pp. 215-224). American Society of Mechanical Engineers.

[10] Picallo-Perez, A., Sala-Lizarraga, J. M., Iribar-Solabarrieta, E., & Odriozola-Maritorena, M. (2016) Application of the Malfunction Thermoeconomic Diagnosis to a Dynamic Heating and DHW Facility for Fault Detection. Energy and Buildings. 135, 385-397.

[11] Verda, V., Serra, L. M., & Valero, A. (2002). Zooming procedure for the thermoeconomic diagnosis of highly complex energy systems. International Journal of Thermodynamics, 5(2), 75-83.

[12] Verda, V., Serra, L., & Valero, A. (2004). The effects of the control system on the thermoeconomic diagnosis of a power plant. Energy, 29(3), 331-359.

[13] Mendes, T., Venturini, O. J., & Pirani, M. J. (2012). Thermodynamic Diagnosis Techniques To Assess The Behavior Of Vapour Compression Refrigeration Systems.

[14] Shi, Y., Xu, J., & Zhou, K. (2009). Structural theory and thermoeconomic diagnosis: application to a supercritical power plant. In 2009 Asia-Pacific Power and Energy Engineering Conference (pp. 1-4). IEEE.

[15] Piacentino, A., & Talamo, M. (2013). Innovative thermoeconomic diagnosis of multiple faults in air conditioning units: Methodological improvements and increased reliability of results. International Journal of Refrigeration, 36(8), 2343-2365.

[16] Piacentino, A., & Talamo, M. (2013). Critical analysis of conventional thermoeconomic approaches to the diagnosis of multiple faults in air conditioning units: capabilities, drawbacks and improvement directions. A case study for an air-cooled system with 120 kW capacity. International Journal of Refrigeration, 36(1), 24-44.

[17] Lazzaretto, A., & Toffolo, A. (2006). A critical review of the thermoeconomic diagnosis methodologies for the location of causes of malfunctions in energy systems. Journal of Energy Resources Technology, 128(4), 335-342.

[18] Reini, M., & Taccani, R. (2004). On the Thermoeconomic Approach to the Diagnosis of Energy System Malfunctions-The Role of the Fuel Impact Formula. International Journal of Thermodynamics, 7(2), 61-72.

[19] Picallo, A., Escudero, C., Flores, I., & Sala, J. M. (2016). Symbolic Thermoeconomics In Building Energy Supply Systems. Energy and Buildings, 127, 561-570.

[20] Valero, A., Correas, L., Zaleta, A., Lazzaretto, A., Verda, V., Reini, M., & Rangel, V. (2004). On the thermoeconomic approach to the diagnosis of energy system malfunctions: Part 2. Malfunction definitions and assessment. Energy, 29(12), 1889-1907.

[21] Usón, S., & Valero, A. (2007). Intrinsic and Induced Malfunctions Quantification in Thermoeconomic Diagnosis Through Quantitative Causality Analysis. Proceedings of ECOS 2007.

[22] Xu, J. Q., Yang, T., Zhou, K. Y., & Shi, Y. F. (2016). Malfunction diagnosis method for the thermal system of a power plant based on thermoeconomic analysis. Energy Sources, Part A: Recovery, Utilization, and Environmental Effects, 38(1), 124-132.

[23] Toffolo, A., & Lazzaretto, A. (2004). On the Thermoeconomic Approach to the Diagnosis of Energy System Malfunctions-Indicators to Diagnose Malfunctions: Application of a New Indicator for the Location of Causes. International Journal of Thermodynamics, 7(2), 41-49.

[24] Energy keys of the housing sector in the Basque Country. Claves energéticas del sector doméstico en Euskadi. EVE. (2013)

[25] Transient System Simulation Tool Trnsys, Thermal Energy Systems Specialists, Madison, USA.(2009)

[26] Lazzaretto, A., & Tsatsaronis, G. (2006). SPECO: a systematic and general methodology for calculating efficiencies and costs in thermal systems. Energy, 31(8), 1257-1289.

A COMPARATIVE ANALYSIS OF TWO THERMOECONOMIC DIAGNOSIS METHODOLOGIES IN A BUILDING HEATING AND DHW FACILITY

Ana Picallo[1], José Mª Sala, Cesar Escudero
Research group ENEDI, Department of Thermal Engineering, University of the Basque Country (UPV/EHU); Alameda Urquijo, S/N, 48013 Bilbao, Vizcaya, Spain.
[1]Corresponding author. E-mail: ana.picallo@ehu.eus

ABSTRACT

Concerning the building environment HVAC facilities, even if a great effort has been made in developing components and systems with high nominal efficiencies, less attention has been paid to the problem of system maintenance.

The main objective of the *thermoeconomic diagnosis* is to detect possible anomalies and their location inside a component of the energy system. The second objective, and indeed the one to be achieved in this paper, is indicated as *inverse problem.* It is associated with the quantification of the effects of anomalies in terms of thermoeconomic quantities. Its rigorous application in building thermal installations has some difficulties relating to the strong interrelation between the different components and the fact that energy supply facilities are continuously changing with time.

The way to deal with *dynamic* circumstances is thoroughly explored in this article.

Likewise, this paper's main goal is to demonstrate an application of two thermoeconomic diagnosis methodologies in the building sector, one based on the *malfunction and dysfunction* analysis and the other one based on the *characteristic curves* of the components. The results obtained allow us to point out the advantages and limitations of both methodologies as well as to combine them and then develop a more reliable diagnosis.

Keywords: Thermoeconomic diagnosis; Dynamic behaviour; Malfunction and Dysfunction; Characteristic curves; Multi-fault.

Highlights: ♦ Detailed dynamic thermoeconomic diagnosis in buildings energy supply system is made ♦ A new way for fault detection and their effects quantification is developed ♦ Two thermoeconomic diagnosis methods are applied ♦ Characteristic curves and MF and DF methods are shown to be complementary ♦ Diagnosis of a multi-fault heating and DHW facility is performed.

1. INTRODUCCTION

In recent years, the construction sector has been in the spotlight of policies focusing on the reduction of primary energy consumption and also oriented in the downsizing of CO_2 emissions. It is estimated that heating, ventilation and air conditioning (HVAC) systems consume about 50% of the total energy used in buildings worldwide. Then by properly operating the HVAC systems, considerable energy savings can be achieved [1].

However, it is not only a matter of designing and sizing the higher performance thermal systems, optimizing its costs and trying to design them for the minimum environmental impact, since its *maintenance* should also be taken into consideration.

Systems are often poorly maintained and experience dramatic degradation of performance due to aging and the presence of malfunctions or faults [2]. Those anomalies do not cause the unit to stop functioning, but they do produce degradation in plant performance that could be the beginning of undesirable induced effects which can seriously damage the nominal operational condition of the facility.

Thermoeconomic diagnosis is focused on discovering reductions in system efficiency, the detection of possible anomalies, the identification of the components where these anomalies have occurred and their quantification [3]. This paper compares two thermoeconomic methodologies in the diagnosis of a heating and DHW supply system, one based on the malfunction and dysfunction method [4] and the other one based on the characteristic curves [5] of the components.

The paper is organized in 6 different sections as follows: after the introductory first section, Section 2 presents the main ideas and sums up the malfunction and dysfunction diagnosis formulas based on the productive structure of the system. In addition, drawbacks of this method are also exposed. Another diagnosis perspective, driven by characteristic curves, is introduced in Section 3 along with the generic formulas. The case study where both diagnosis methodologies are implemented is defined in Section 4. The application of both methods of diagnosis and the numerical results obtained are covered in Section 5. Finally, the main contributions of the paper and the discussions on the results are summarized in Section 6.

MATRICIAL NOMENCLATURE

- $\mathbf{X}$ (nx1) Generic vector of X variable
- $\mathbf{X_D}$ (nxn) Diagonal matrix of X vector
- $\mathbf{X^0}$ (nx1) Reference condition of generic X vector
- $\mathbf{\Delta X}$ (nx1) Variation of generic X vector between two conditions
- $\mathbf{{}^tX}$ (1xn) Transposed of generic X vector
- $\mathbf{u}$ (nx1) Unitary vector
- $X^{1^{st}}, X^{2^{nd}}$ (1x1) generic value of X for the 1st and 2nd diagnosis calculation

MF & DF ANALISYS

- $\mathbf{P}$ (nx1) Component Product vector
- $\mathbf{P_S}$ (nx1) Final product vector
- $\mathbf{K}$ (nx1) Unit exergy consumption vector
- $\boldsymbol{\kappa_0}$ (nx1) Vector of the marginal exergy consumptions related to the external resources
- $\langle\mathbf{KP}\rangle$ (nxn) Matrix of the marginal exergy consumptions, κ_{ij}
- $|\mathbf{I}\rangle$ (nxn) Matrix irreversibility extended operator
- F_T, F_T^0 (1x1) Resource consumption in real and reference operating conditions
- $\mathbf{MF}$ (nx1) Malfunction vector
- $\mathbf{DF}$ (nx1) Dysfunction vector
- DF_{ij} (−) Components of the Dysfunction matrix

CHARACTERISTIC CURVES

- π (1x1) Generic term for characteristic curves representation
- ξ (1x1) Subset of generic independent variables
- κ (1x1) Specific term for characteristic curves application
- τ (1x1) Subset of specific thermal independent variables
- $\kappa_{i,ind}^{0}$ (1x1) Induced unit exergy consumption of the i^{th} component
- $MF_{i,ind}$ (1x1) Induced malfunction of the i^{th} component
- $MF_{i,int}$ (1x1) Intrinsic malfunction of the i^{th} component

Figure 1: Nomenclature and brief description of symbols grouped according to their purpose

2. THERMOECONOMIC DIAGNOSIS. MF & DF ANALYSIS

General Characteristics

Thermoeconomics relates the thermodynamic parameters with the economic ones based on the idea that *exergy* is the unique parameter which rationally determines the cost of the fluxes; this is due to the fact that exergy takes into account the quality of energy and the irreversible nature of energy conversions [6].

Beyond that, thermoeconomic analysis is based on the *productive structure* [7] of the plant where the interactions between components are identified according to their functional relationships. The exergy flows related to the component resources are labelled as *Fuel*, F, whereas those associated with the desired output are known as *Product*, P, which meanwhile, can be fuel from other components and sometimes from wastes or residues. Components are described by their specific exergy consumptions which refer to the amount of resources needed to produce a unit of product, and this parameter being one of the key variables for diagnosis purposes.

Thermoeconomic diagnosis is difficult to apply in building HVAC systems, precisely because:

- It should be noted that exergy is always evaluated with respect to a reference environment, *dead state*. Exergy methods applied in buildings might seem cumbersome or complex to some people, since not only is a dead state difficult to define but it also changes dynamically over time, and the results might seem difficult to interpret and understand [8].
- The definition of *productive structure* may well lead to controversy [9] due to the dynamic behaviour of thermal installations in buildings. The same system can have more than one productive structure depending upon the switching on and switching off of the components. Likewise, the performance of any component, in fact, is heavily influenced by all other components because of the system

balancing; then, the effects of any anomaly will propagate to the whole plant, due to the complex relationships.

- The most challenging enforcement of thermoeconomic diagnosis is to resolve the *direct problem,* which consists of detecting a possible anomaly and its location. It is a difficult task and the reliability of its results has not yet been proven [10]. For the moment, only the *inverse problem* of diagnosis has been solved, i.e., under the *knowledge* of specific anomalies in different components, the procedure involves quantifying the effects of those anomalies in terms of thermoeconomic quantities, such as fuel impact and malfunctions.

Nevertheless, several thermoeconomic diagnoses have been published during the last years, although most of them are applied to industry. Verda and his co-workers applied a zooming strategy in a combined cycle in order to first locate the macro-component where the anomaly occurs [9], [11]. Besides that, this same author also developed a methodology in which the effects of the control system are filtered [12]. Mendes et al [13] analysed the influence of two different mono-fault cases implemented in a vapour compression refrigeration system, whereas Shi et al [14] discussed the fuel impact that results from malfunctions that occur when two LP heaters are out of service in a 1000 MW supercritical power plant. Piacentino and Talamo [15] proposed an improved thermoeconomic diagnosis method and applied it in a 120 kW air conditioning system and these same authors [16] made a critical analysis on the capabilities and the limits of thermoeconomic diagnosis in a multiple simultaneous faults air-cooled air conditioning system. Finally, it is worth highlighting the study where the effects produced by a mono-fault located on the radiators system of a DHW and heating demand facility is addressed [10].

Malfunction and Dysfunction Analysis

As a brief summary, the diagnosis method is based on the comparison between the real (malfunctioning) and reference (without anomalies) operating conditions. Different indicators can be used to quantify the effects of malfunctions [17]. The additional fuel consumption ΔF_T, or *fuel impact* [18], is the difference between the resource consumption of the plant in operation and in the reference condition:

$$\Delta F_T = F_T - F_T^0 \qquad 1)$$

From that representation, the fuel impact formula can be extended and related to every component as the sum of malfunctions MF_i, dysfunctions DF_i and the final product variation ΔP_{s_i}:

$$\Delta F_T = {}^t\mathbf{u}\cdot[\mathbf{MF} + \mathbf{DF} + \mathbf{\Delta P_S}] \qquad 2)$$

Malfunction in i^{th} component, MF_i, occurs due to an increase of the unit exergy consumption $\Delta\kappa_i$ in the component itself; and DF_i is the variation of the i^{th} component production induced by intrinsic malfunctions in other components. So dysfunctions are not related to a variation of the component efficiency, i.e. they can occur in components whose exergy efficiencies have maintained constant. They are defined as follows [10]:

$$\mathbf{MF} = \mathbf{\Delta K_D}\cdot\mathbf{P^0} \qquad 3)$$

$$\mathbf{DF} = (\mathbf{K_D} - \mathbf{U_D})\cdot\mathbf{\Delta P} \qquad 4)$$

As it will be explained later on, eq(3) and eq(4) can be estimated independently at the component level; this is to say, without considering the relationships between the elements inside the system.

Nevertheless, in addition to this representation, as the distribution of the resources throughout the plant and the interconnections among subsystems are defined by the productive structure, MF and DF analysis can be understood as follows [10]:

$${}^t\mathbf{MF} = {}^t\boldsymbol{\Delta\kappa_0}\cdot\mathbf{P_D^0} + {}^t\mathbf{u}\cdot\left(\boldsymbol{\Delta}\langle\mathbf{KP}\rangle\cdot\mathbf{P_D^0}\right) \qquad 5)$$

$$\mathbf{DF} = |\mathbf{I}\rangle\cdot\mathbf{\Delta P_s} + \left(|\mathbf{I}\rangle\cdot\boldsymbol{\Delta}\langle\mathbf{KP}\rangle\cdot\mathbf{P_D^0}\right)\cdot\mathbf{u} \qquad 6)$$

were $\Delta\kappa_0$ contains the variation of the marginal exergy consumption associated with the external resources; and $\Delta\langle KP\rangle$ refers to the variation of the marginal exergy consumption of each component (i.e. $\Delta\kappa_{ij}$ accounts the portion of *j* total resources coming from *i* product for the obtainment of a unit of *j* product), whereas $|\mathbf{I}\rangle$ refers to the irreversibility extended matrix operator [19].

In this way, by interpreting the dysfunction matrix **DF**, the induced dysfunction can be related to the malfunction that generates it and to that fostered by $\mathbf{\Delta P_s}$. That is to say, DF_{ij} picks out the dysfunction part of *i* caused by a malfunction in *j* and DF_{i0} reflects the induced consumption variation boosted by the final product variation.

If the reader wants to delve more deeply into diagnosis roots and its mathematical development, the paper [19] together with [10] illustrate the direct way to achieve that aim.

Shortcomings of this method

Although this formula seems very attractive, the contributions given by the malfunction terms should not be confused with the effects due to the *intrinsic malfunctions*, since the variations of unit exergy consumption can be caused by *induced* perturbations as well; or similarly stated, the term $\Delta\kappa_i = \sum_j \Delta\kappa_{ij}$ does not only represent the consumption variation due to an intrinsic anomaly in the i^{th} component but it is also owed to the effects prompted by other components anomalies. Consequently, the contributions given by the terms DF represent only a part of the overall induced effects [17].

Henceforth, induced effects must be detected for a proper study. These effects take place when a component without anomalies works at a non-reference operating condition.

According to [20], malfunctions can be categorized as either internal or external and then distributed in some subcategories. In Figure 2 each type is labelled and shortly explained.

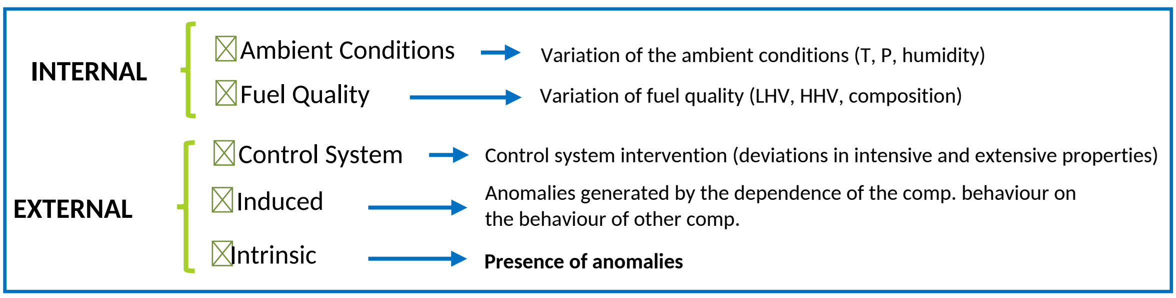

Figure 2: Malfunction Classification

Because different malfunctions take place during a faulty operating condition, and in order to make a reliable diagnosis, the influence of induced effects should be distinguished from the intrinsic ones:

- *External effects* are easily avoided by imposing the same ambient conditions and same fuel quality in both the faulty and reference operating condition.
- *Control system intervention* imposes some barriers to the malfunction propagation which can also be prevented. The effect of an anomaly in a component generally induces a variation in the thermodynamic properties of the downstream flows, but the control system, commanded by some restrictions, acts with the aim of adapting to the new circumstances [12]. This control effect should be filtered to properly compare reference and real faulty operating conditions so that both cases have an equivalent behaviour. An artificial condition is obtained by restoring the same reference regulation condition in the faulty one, known as *free condition*, which should be virtually determined, as is described in [10].
- The main difficulty of this task is the presence of *induced malfunctions*, which appear because unit exergy consumptions are not true independent variables. Some components may present a reduced efficiency, although they are not sources of operating anomalies, due to non-flat efficiency curves. In Lazzaretto and co-workers opinion [17], a rigorous *mathematical* approach based on the true independent variables of the system is therefore required.

As the malfunction and dysfunction analysis does not discriminate between intrinsic and induced malfunctions, it cannot be considered a fully reliable approach. This methodology is effective in the evaluation of the malfunction effects but not in identifying the sources of anomalies.

3. THERMOECONOMIC DIAGNOSIS. CHARACTERISTIC CURVES

General Characteristics

Regarding the objective of searching a rigorous mathematical approach to distinguish induced effects from intrinsic ones, some authors have developed different theories based directly on the thermodynamic description of the model. For instance, Uson and Valero [21] provide a systematic numerical decomposition of malfunctions and malfunction costs into intrinsic and induced effects relying on thermodynamic restrictions of the problem, but unfortunately, it is not a direct procedure. Xu and al. [22], however, based their study on a new indicator proposed by Toffolo and Lazzaretto [23] which accords to the availability of component *characteristic curves* in the reference operating conditions.

The characteristic curves of a i^{th} component consist of a set of relationships expressing a thermodynamic quantity π_i that characterizes the component behaviour as a function of some variables ξ_i involved in the component operation. The generic characteristic curve associated with the reference operating condition takes the form of eq(7) and a specific working point (R) inside that curve is represented by eq(8):

$$\pi_i^0 = f^0\left(\xi_i^0\right) \quad 7)$$
$$\pi_i^{0,R} = f^0\left(\xi_i^{0,R}\right) \quad 8)$$

The selected thermodynamic parameter representing the component π_i can be different depending on the chosen criteria. Toffolo and Lazzaretto [23] recommend component *irreversibility* because then the indicator takes a strictly positive value in case there is a presence of anomalies. Nevertheless, in order to make a direct comparison with the previous diagnosis method, the dependent thermodynamic quantity to express will be the component unit exergy consumption, κ_i. The variables ξ_i chosen for these curves are the mass flow rates, temperatures and pressures, designated as τ_i. Hence, the appearance of the generic characteristic curve used for reference condition eq(9) and its specific working point (R), eq(10), are:

$$\kappa_i^0 = f^0\left(\tau_i^0\right) \qquad 9)$$

$$\kappa_i^{0,R} = f^0\left(\tau_i^{0,R}\right) \qquad 10)$$

Let us now assume that because the induced effects are transferred downstream, the $\tau_i^{0,R}$ values change according to the physical constraints imposed by the component characteristic to $\tau_i^{0,A}$. Therefore, the component will be working in a new operating condition point, A, but still, the point will belong to the reference condition characteristic curve, f^0:

$$\kappa_i^{0,A} = f^0\left(\tau_i^{0,A}\right) \qquad 11)$$

Moreover, let us consider a new situation where the component contains an anomaly, which means the presence of an intrinsic malfunction. In this case again, the component will be in a different working point, B, with different independent variable values, τ_i^B. But nonetheless, since the i^{th} component contains a fault, the characteristic curve connected to faulty condition f would be different from the reference one, f^0:

$$\kappa_i^B = f\left(\tau_i^B\right) \qquad 12)$$

Characteristic Curves Application

This study needs to be individually implemented in each component. As said above, the generic i^{th} component would have two values for its unit exergy consumption, one associated with the reference condition κ_i^0, and the other one with the faulty operating condition κ_i.

According to what was previously explained, even if the component does not contain any anomaly, the independent thermal variables in reference condition $\tau_i^{0,R}$ would be different from those on faulty operating condition τ_i^B, due to induced effects. If the i^{th} component contains a fault, the characteristic curve connected to faulty condition f would be different from reference curve f^0. In that case, a new unit exergy consumption value can be calculated eq(13); this is mathematically obtained by inserting the values of the independent variables of faulty operating conditions in the reference characteristic curve.

$$\kappa^{0}_{i,ind} = f^0\left(\tau^{o,A}_i\right) \qquad 13)$$

Figure 3 depicts the three cases.

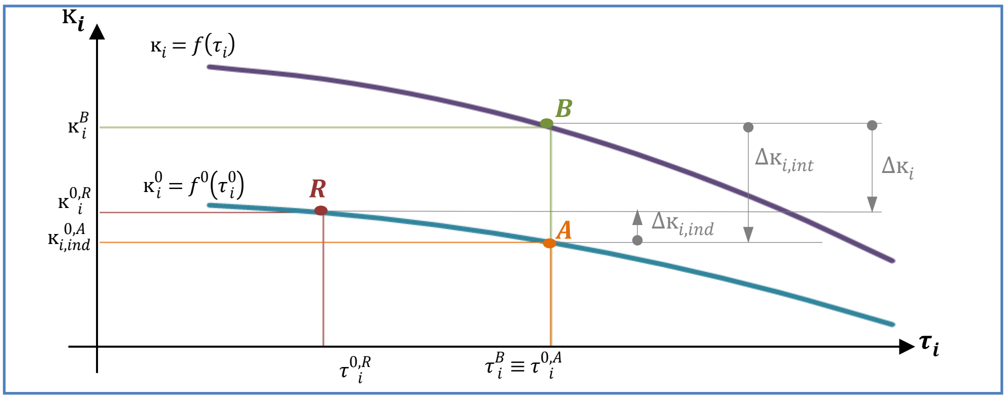

Figure 3: Unit exergy consumption in reference and operating

As a result, the increase of the unit exergy consumption, $\Delta\kappa_i$, can be divided into induced and intrinsic unit exergy consumption variation, $\Delta\kappa_{i,ind}$, $\Delta\kappa_{i,int}$, as follows:

$$\Delta\kappa_{i,ind} = \kappa^0_{i,}\left(\tau^A_i\right) - \kappa^0_i\left(\tau^R_i\right) \qquad 14)$$

$$\Delta\kappa_{i,int} = \kappa_i\left(\tau^B_i\right) - \kappa^0_i\left(\tau^A_i\right) \qquad 15)$$

Consequently, according to eq(3) the malfunction of each component can be expressed as the sum of intrinsic and induced malfunctions:

$$MF_i = MF_{i,int} + MF_{i,ind} = \Delta\kappa_{i,int}\cdot P^0_i + \Delta\kappa_{i,ind}\cdot P^0_i \qquad 16)$$

This formulation allows calculating individually the effects that anomalies produce in every component depending on the thermodynamic independent variables.

A generic procedure is therefore established to locate the origin of system intrinsic and induced malfunctions from the analysis of the faulty operating conditions, where the only possible source of uncertainty is the inaccuracy in the reconstruction of component characteristic curves, due to the required amount of data.

Revision of both Methodologies

Both techniques of thermoeconomic diagnosis give different essential information:

- Malfunction and dysfunction diagnosis procedure uses the Fuel-Product productive structure in order to relate each component inputs and outputs to the rest of the subsystems. It does not differentiate between intrinsic and induced malfunction but, the dysfunctions provoked by j belonging to a malfunction in i can be estimated, as well as those generated due to the final production variations. Likewise, the way that the whole plant efficiency changes when the efficiency of any component varies can also be easily calculated. Moreover, as the productive structure is also used for cost accounting, either the *exergetic cost* or the *economic cost* of every flow and of the overall system can be assessed as well [19], in addition to the *cost impact* generated by the anomalies [10].
- Characteristic curves change the perspective and refer to the components individually. This method enables researchers to distinguish between the induced and intrinsic malfunctions in every component by considering the actual links among the thermodynamic variables (pressure, temperature mass flows and composition) and the exergy unitary consumptions.

Combination of both methodologies . Fault detection approach

Supposing that *more than one* intrinsic malfunction has taken place in the system, the MF and DF diagnosis is not able to furnish any information about the incidence of each one on the total fuel impact, since the irreversibility variation causes a different fuel impact depending on the position of the component where the fault has occurred.

When various anomalies appear in the system, each anomaly would induce effects in the j^{th} component with the anomaly itself, varying its $\Delta\kappa_{j,int}$ (intrinsic malfunction) and in the rest of i^{th} components varying both the unit exergy consumption, $\Delta\kappa_{i,ind}$ (induced malfunctions), and the local production, ΔP_i (dysfunctions). The objective is to distinguish between the $\Delta\kappa_{i,ind}$ and ΔP_i produced by each anomaly so the extra consumption can be attributed to the j^{th} malfunctioning component which has generated them. Thanks to the MF and DF diagnosis, this last extra consumption provoked by j related to the ΔP_i variation is accounted for through DF_{ij}, but further information is needed for accounting the remaining induced malfunction effects.

Consequently, if the information acquired by this diagnosis is complemented with the characteristic curves analysis, the subsystem with higher intrinsic malfunction can be recognized and identified as the faultiest component. However, even now, the extra consumption caused by $\Delta\kappa_{i,ind}$ cannot be attributed to any component, nor can the one belonging to the final production variation ΔP_s, because this analysis is individually performed and the induced effects could have been caused by more than one different component.

Notwithstanding these barriers, thanks to characteristic curves analysis, the component identified as the faultiest one (let's say j component) can be virtually erased and a second diagnosis study can be executed. In this way, the decrease of the fuel impact accounted from the first study, $\Delta \mathrm{F}^{1^{st}}_{T}$, to the next one , $\Delta \mathrm{F}^{2^{nd}}_{T}$, would express the savings gained when the anomaly in j is repaired:

$$\Delta F_{save} = \Delta \mathrm{F}^{1^{st}}_{T} - \Delta \mathrm{F}^{2^{nd}}_{T} \qquad 17)$$

In the same way, that ΔF_{save} would correspond to the sum of the intrinsic malfunctions in j $\left(MF^{1^{st}}_{j,int}\right)$ and its induced effects calculated in the first study $\left(\sum_i DF^{1^{st}}_{ij} + \sum_i MF^{1^{st}}_{ij,ind}\right)$ plus the final production variation $\left(\Delta\Delta P^{1^{st},2^{\mathrm{nd}}}_{s}\right)$ and the dysfunction it generates between both situations $\left(\Delta DF^{1^{st},2^{\mathrm{nd}}}_{0}\right)$:

$$\Delta F_{save} = \left[MF^{1^{st}}_{j,int} + \sum_i DF^{1^{st}}_{ij} + \sum_i MF^{1^{st}}_{ij,ind}\right] + \left[\left(DF^{1^{st}}_{o} - DF^{2^{nd}}_{0}\right) + \left(\Delta P^{1^{st}}_{s} - \Delta P^{2^{nd}}_{s}\right)\right] \qquad 18)$$

As $MF^{1^{st}}_{j,int}$, $\Sigma_i DF^{1^{st}}_{ij}$ and $DF^{1^{st},2^{nd}}_{0}$, $\Delta P^{1^{st},2^{nd}}_{s}$ are calculated through one of the above methodologies, $\Sigma_i MF^{1^{st}}_{ij,ind}$ can be easily obtained with a simple subtraction.

If this is repeated as many times, or steps, as intrinsic malfunctions exist, the diagnosis inverse problem is solved. Figure 4 outlines the methodology routine.

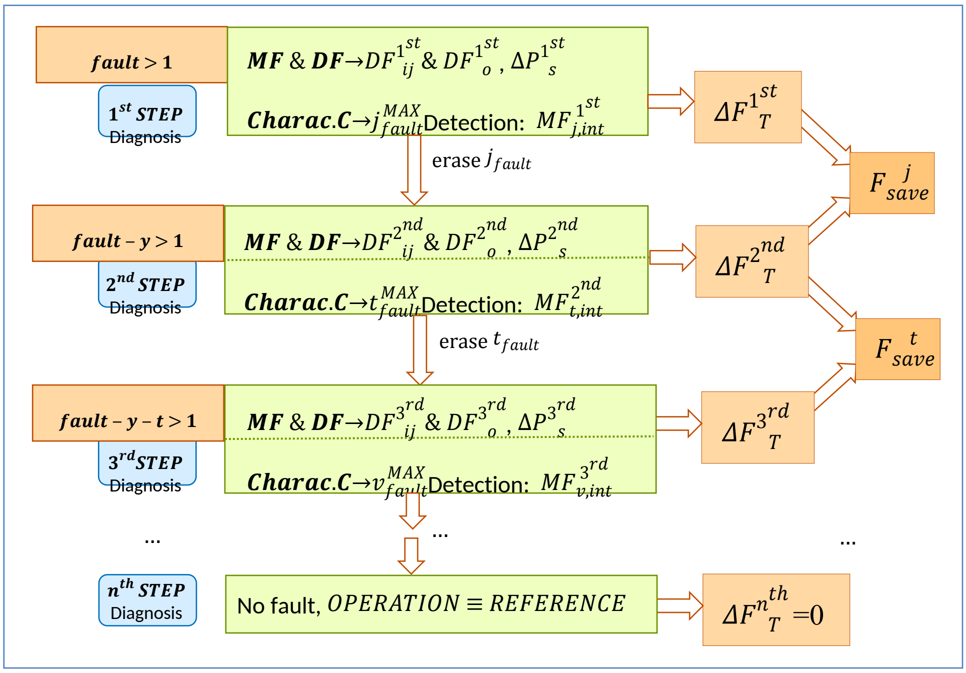

Figure 4: Diagnosis methodology through the combination of MF&DF study and characteristic curves

4. DYNAMIC CASE STUDY

Preliminary work

The two diagnosis methods presented above will be applied in a heating and DHW plant in order to highlight its characteristics, compare both methodologies and complement them in a *dynamic building environment.* Let's assume there is a *multi-fault* case where some anomalies are intentionally introduced.

First of all, it is recommended to highlight that research on building thermal facilities implies *dynamic studies* according to the changing behaviour of the variables such as climate, user demand and so on, which directly interferes in the start-up and shutdowns of the elements integrated in the installation. On the other hand, as diagnosis involves the *comparison* between two operating conditions, dynamic simulation of the faulty (with anomalies) and the reference conditions needs to be done, while in both the heating and the DHW demand should be kept the same.

As previously stated, the ambient conditions during the heating season coincide in both simulations, as well as the fuel quality and composition; the control system intervention effect is avoided through the free condition obtainment which is fully explained in [10]. Because of the free condition achievement and due to the arguments displayed in [10], a DHW production output variation would inevitably exist $\Delta P_{s_{DHW}} \neq 0$, being indeed $\Delta P_{s_{DHW}} < 0$.

The simulation is done with a 30s time-step and the reference operating condition data and free condition data (named as faulty condition) is extracted every *hour* during the heating season. So the dynamic study is represented as a set of hourly quasi-static states joined by one after the other.

General description of the facility

The reference generic facility coincides with the one used in [10], where a full explanation of all components can be found; additionally, in this case, the pumps are considered in the study. The system covers the heating and DHW demand of a 16 householder multi-family flat located in Bilbao (Spain), through a typical heating installation in the Basque Country [24].

As a general explanation, the energy supply system consists of a 28 kW natural gas boiler. Other components are a 35 litter hydraulic compensator, three way valves, a heat exchanger and a 1000 litter DHW storage tank, see Figure 5; the heating demand is represented through the heat dissipation of a radiator system and a 3-way valve. The DHW is given by a DHW tank and a 3-way valve that ensures hot water at a constant temperature.

As extensively explained in [26], before any calculation a decision must be made with respect to whether the analysis of the components should be conducted using total exergy or separate forms of it (i.e. thermal, mechanical and chemical exergies). Even if splitting the exergy refines the accuracy, the computational efforts are much higher than the obtained improvements; the corrections are often marginal and they are not necessary for extracting the main conclusions from the exergoeconomic diagnosis evaluation. For that reason, the total exergy will be considered in the research.

Overall a total of 13 components were listed and described in Table 1, and 28 flows were considered for the study, as seen in Figure 5. Different inputs coming from three external

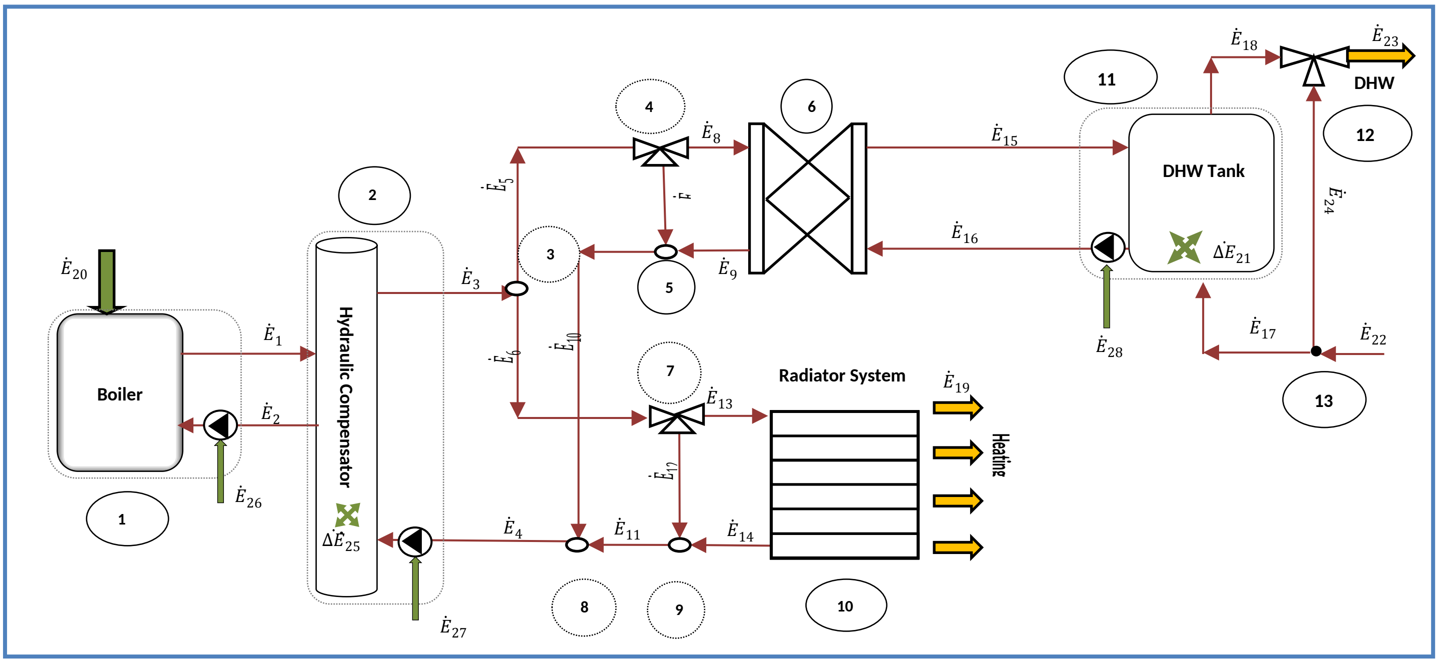

Figure 5: Physical Structure of the facility

sources are noted: (1) natural gas ($\dot{E}_{20}$), (2) the contribution given by the hydraulic compensator ($\Delta\dot{E}_{25}$) and the tank ($\Delta\dot{E}_{21}$), which are the difference between the initial and final exergy those components have in the considered period, and (3) three inputs coming from the electrical grid, one for powering each pump ($\dot{E}_{26}$,$\dot{E}_{27}$, $\dot{E}_{28}$). Those are represented by green arrows whereas yellow arrows indicate the final products leaving the system, such as DHW ($\dot{E}_{23}$) and heating demand ($\dot{E}_{19}$).

The various components appearing in the case study are simulated using simplified models available from the Trnsys v17 library. The *control* that turns on and deactivates the devices of the plant is insightfully detailed in [10].

Thermoeconomic Diagnosis

As mentioned, the dynamic simulation will provide the hourly data required for the calculation of every exergy flow $\dot{E}_i$ eq(20). Then, a thermodynamic diagnosis will be completed hourly by eq(5) and eq(6) and afterwards, the malfunctions and dysfunctions accumulated at the end of the studied period will be calculated. Consequently, the fuel impact according to the incorporation of those anomalies is also quantified.

The first and probably the most sensitive step for this analysis is defining the productive structure for each time-step following the pattern given in [19]. As previously remarked, the system dynamic behaviour interferes in the start-up and shutdowns of the components, so that the productive structure varies depending on the components which are turned on in that precise moment. Figure 6 illustrates two of the possible cases: case 1 depicts the situation where only DHW demand is requested; case 2 shows the situation where only heating demand is claimed. Both cases are associated with two different productive structures.

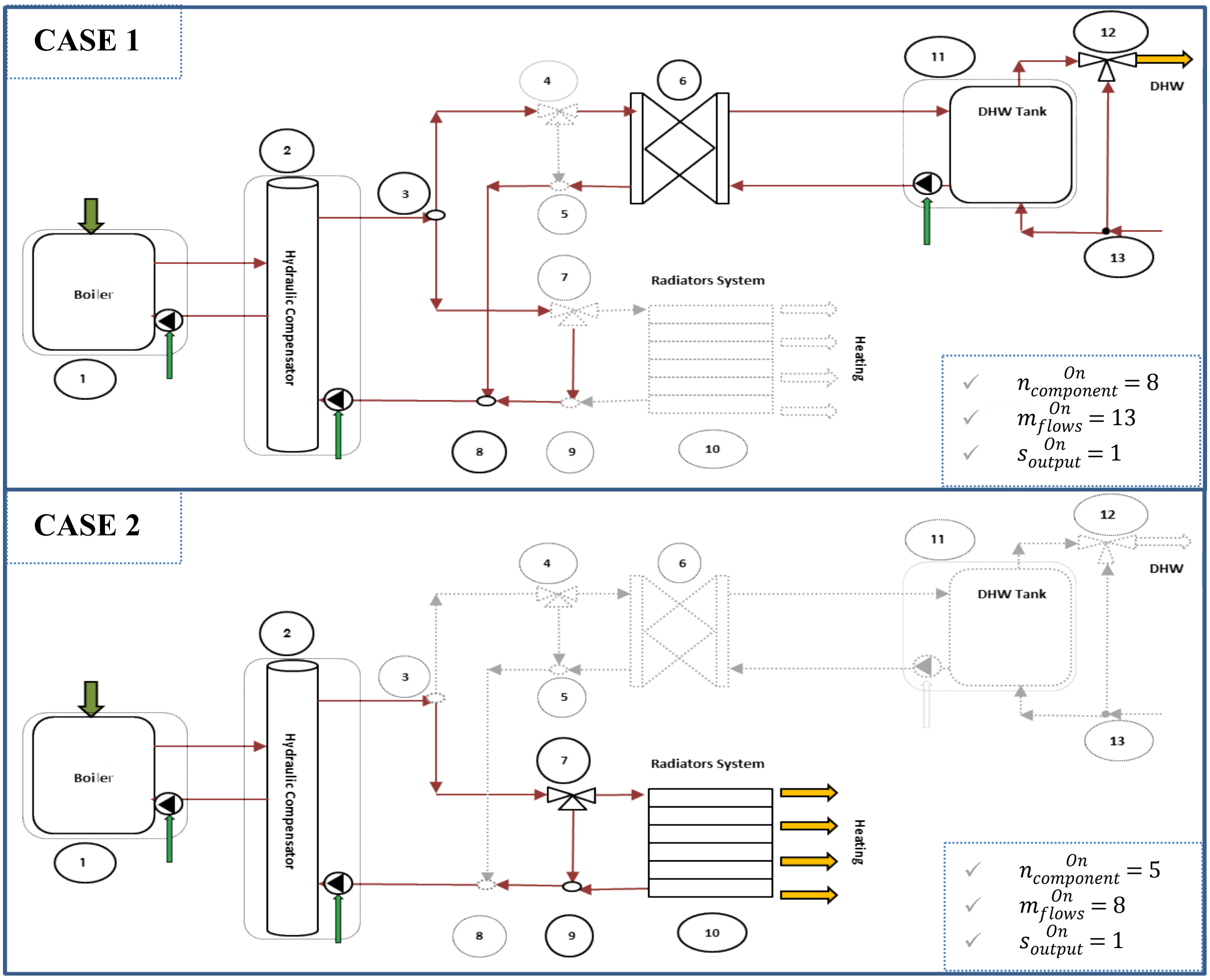

Figure 6: Different operation situations related to different productive structures

Although all the components do not have to be simultaneously switched on, Table 1 specifies F, P and κ for every component according to the nomenclature in Figure 5.

Table 1: F/P Table and exergy unitary consumption of each subsystem

n	COMPONENT		F_i	P_i	κ_i
①	Cond. Boiler + Gen. Pump	CB	$\dot{E}_{20}$	$\dot{E}_1 - \dot{E}_2$	$\dot{E}_{20}/(\dot{E}_1 - \dot{E}_2)$
②	Compensator + Dist. Pump	HC	$(\dot{E}_1 - \dot{E}_2) + \Delta\dot{E}_{25}$	$\dot{E}_3 - \dot{E}_4$	$[(\dot{E}_1 - \dot{E}_2) + \Delta\dot{E}_{25}]/(\dot{E}_3 - \dot{E}_4)$
③	Heating & DHW Diverter	D1	$\dot{E}_3$	$\dot{E}_5 + \dot{E}_6$	$\dot{E}_3/(\dot{E}_5 + \dot{E}_6)$
④	DHW 3-way valve	V1	$\dot{E}_5$	$\dot{E}_7 + \dot{E}_8$	$\dot{E}_5/(\dot{E}_7 + \dot{E}_8)$
⑤	DHW Mixer	M1	$\dot{E}_7 + \dot{E}_9$	$\dot{E}_{10}$	$(\dot{E}_7 + \dot{E}_9)/\dot{E}_{10}$
⑥	Heat Exchanger	HX	$\dot{E}_8 - \dot{E}_9$	$\dot{E}_{15} - \dot{E}_{16}$	$(\dot{E}_8 - \dot{E}_9)/(\dot{E}_{15} - \dot{E}_{16})$
⑦	Heating 3-way valve	V2	$\dot{E}_6$	$\dot{E}_{12} + \dot{E}_{13}$	$\dot{E}_6/(\dot{E}_{12} + \dot{E}_{13})$
⑧	Heating & DHW Mixer	M2	$\dot{E}_{10} + \dot{E}_{11}$	$\dot{E}_8$	$(\dot{E}_{10} + \dot{E}_{11})/\dot{E}_8$
⑨	Heating Mixer	M3	$\dot{E}_{12} + \dot{E}_{14}$	$\dot{E}_{11}$	$(\dot{E}_{12} + \dot{E}_{14})/\dot{E}_8$
⑩	Radiators System	RS	$\dot{E}_{13} - \dot{E}_{14}$	$\dot{E}_{19}$	$(\dot{E}_{13} - \dot{E}_{14})/\dot{E}_{19}$
⑪	DHW Tank + Storg. Pump	T	$(\dot{E}_{15} - \dot{E}_{16}) + \Delta\dot{E}_{21}$	$\dot{E}_{18} - \dot{E}_{17}$	$[(\dot{E}_{15} - \dot{E}_{16}) + \Delta\dot{E}_{21}]/(\dot{E}_{18} - \dot{E}_{17})$
⑫	DHW 3-way valve	V3	$\dot{E}_{18} + \dot{E}_{24}$	$\dot{E}_{23}$	$(\dot{E}_{18} + \dot{E}_{24})/\dot{E}_{23}$
⑬	DHW Diverter	D2	$\dot{E}_{22}$	$\dot{E}_{17} + \dot{E}_{24}$	$\dot{E}_{22}/(\dot{E}_{17} + \dot{E}_{24})$

Characteristic curves Diagnosis

As previously pointed out, building facilities are strictly linked to dynamic fluctuations. At every time-step the thermodynamic variables τ change so the unit exergy consumption κ of every component also varies. This means that, in the same way as for the earlier method, the study should be repeated for each component individually for every hour during the whole heating season. Afterwards, as in the previous diagnosis, the cumulative values of malfunctions and dysfunctions drawn through this representation will be accounted for using eq(3) and eq(4).

As there are 13 components, at least 13 characteristic curves must be defined. The main goal is to define a curve which recreates the same component behaviour as the one in the previous diagnosis, which is based on the Trnsys v17 algorithm. For that purpose, the Trnsys component mathematical reference guidebook [25] together with its Fortran programming have been analysed. In such way, the independent variables τ_i and physical specific characteristics of every component have been considered. As an example, here there is an explanation as to how to calculate the heat exchanger characteristic curve:

One needs to bear in mind the definition of its unit exergy consumption, which is written in Table 1:

$$\kappa_6 = \frac{\dot{E}_8 - \dot{E}_9}{\dot{E}_{15} - \dot{E}_{16}} \qquad 19)$$

The formula for the generic physical i water exergy flow is expressed as follows:

$$\dot{E}_i = c_P \cdot \dot{m} \cdot T_i - T_0 - T_0 \cdot ln\left(\frac{T_i}{T_0}\right) \qquad 20)$$

were c_p is the fluid specific heat, $\dot{m}$ is the mass flow rate and T_0 refers to the ambient temperature.

The independent variables τ_6 and physical characteristics chosen for the heat exchanger are the primary and secondary inlet temperatures (T_8,T_{16}) (which are likewise outputs of V1 and T), the mass flow rates ($\dot{m}_{prim}$,$\dot{m}_{sec}$), the ambient temperature (T_0) and the overall heat transfer coefficient UA. So that (T_9,T_{15}) output temperatures depend on those variables.

In order to calculate them, the Trnsys heat exchanger algorithm relies on the effectiveness approach: the model starts determining whether the primary or the secondary side is the minimum capacitance side:

$$C_{prim} = c_P \cdot \dot{m}_{prim} \qquad 21)$$
$$C_{sec} = c_P \cdot \dot{m}_{sec} \qquad 22)$$
$$C_{max} = \max\left(C_{prim}, C_{sec}\right) \qquad 23)$$
$$C_{min} = \min\left(C_{prim}, C_{sec}\right) \qquad 24)$$

After that, it calculates the effectiveness based upon the specified flow configuration and on UA:

$$\varepsilon = \frac{1 - e^{\left(-\frac{UA}{C_{min}} \cdot \left(1 - \frac{C_{min}}{C_{max}}\right)\right)}}{1 - \frac{C_{min}}{C_{max}} \cdot e^{\left(-\frac{UA}{C_{min}} \cdot \left(1 - \frac{C_{min}}{C_{max}}\right)\right)}} \qquad 25)$$

Following this trajectory, the heat exchanger outlet temperatures are computed, which would be at the same time the input parameters of M1 and T.

$$T_9 = T_8 - \varepsilon \cdot \left(\frac{C_{min}}{C_{prim}}\right) \cdot (T_8 - T_{16}) \qquad 26)$$

$$T_{15} = T_{16} + \varepsilon \cdot \left(\frac{C_{min}}{C_{sec}}\right) \cdot (T_8 - T_{16}) \qquad 27)$$

In this way κ_6 can be calculated and plotted. Figure 7 depicts the behaviour of κ_6 when one of its independent variables changes its value while the others remain constant.

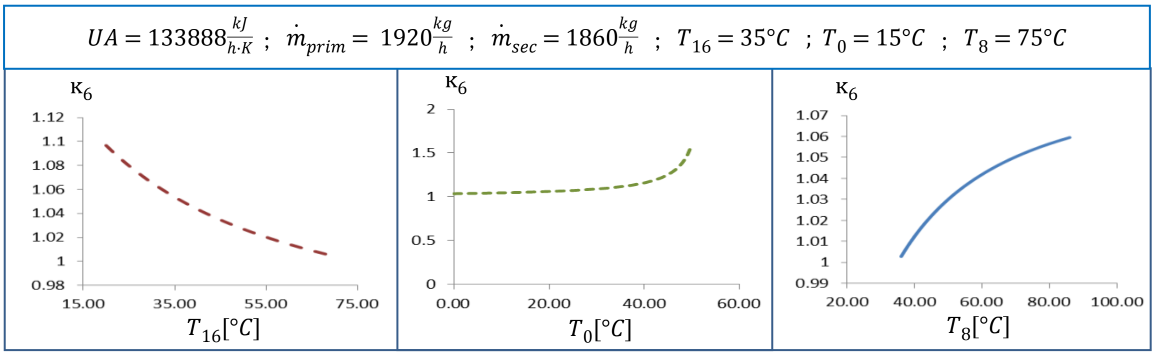

Figure 7: Heat exchanger characteristic curves related to the fluctuation of one independent variable

5. NUMERICAL EXAMPLE

The DHW and space heating energy demand are calculated in the same way as in [9] both accounting for the whole heating season comprising from the 1st of November until the 30th of April.

Multi-Faults

As any component can be chosen for containing the fault and the effects that it would produce depending on the location of that component, two faults are deliberately incorporated on the *radiator system* and *heat exchanger* by degrading some of their physical characteristics. An anomaly is set through a 10% reduction in the RS *energy performance*; and in HX the *overall heat transfer coefficient* is diminished 35%. The reference and operation condition simulation are independently undertaken.

Figure 8 depicts the reference and faulty operation characteristic curves of those components when one of their independent variables changes its value while the rest remain constant.

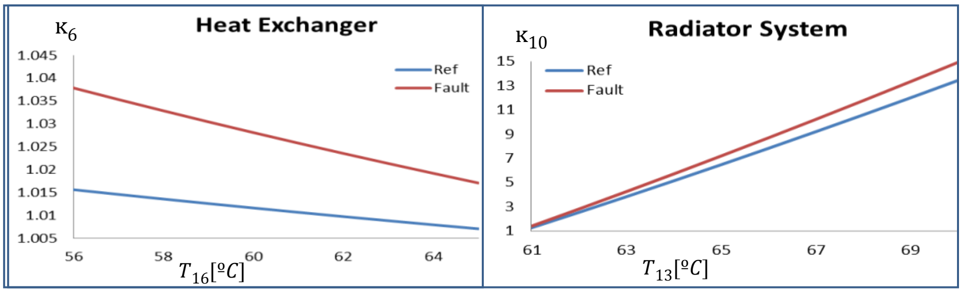

Figure 8: Characteristic curves of reference and faulty components

Simulation and a calculation of the exergy flows are performed hourly. For their calculation, hourly ambient conditions are taken as *dead state* so, dynamic values are regarded. Table 2 is afterwards built, where the accumulated exergy of every flow at the end of the simulation period for reference and faulty operating conditions can be seen.

Table 2: Accumulated exergy values for reference and faulty operating condition $[GJ_{ex}]$

$[GJ]$	E_1	E_2	E_3	E_4	E_5	E_6	E_7	E_8	E_9	E_{10}	E_{11}	E_{12}	E_{13}	E_{14}
Ref.	122.9	100.1	372.3	351.8	192.0	180.3	153.3	38.9	29.8	182.9	169.2	57.6	122.7	111.6
Fault	122.9	99.2	369.8	348.4	190.7	179.1	151.9	38.8	29.8	181.7	166.7	57.7	121.4	109.2

E_{15}	E_{16}	E_{17}	E_{18}	E_{19}	E_{20}	ΔE_{21}	E_{22}	E_{23}	E_{24}	ΔE_{25}	E_{26}	E_{27}	E_{28}
37.2	28.3	0.2	6.5	2.3	149.1	0.04	0.2	5.8	0.03	0.0	1.7	5.9	0.5
36.2	27.5	0.2	6.4	2.3	155.3	0.05	0.2	5.6	0.03	0.0	1.7	5.9	0.5

Thermoeconomic Diagnosis

At first, an hourly MF and DF diagnosis with two faults is carried out and the values obtained are accumulated later on, see Table 3. The first column identifies each component with its corresponding number. The second column contains the malfunction, MF_i, of every component, eq(5). The expanded dysfunction matrix comes next where the dysfunction according to the exergy consumption variation associated with the external resources, DF_0, and the other components, DF_{ij}, are reflected, eq(6). The last column corresponds to the final product variation, according to eq(2).

Table 3: MF and DF tables extracted from diagnosis accumulation $[\boldsymbol{MJ}]$

MF & *DF* 1^{st} DIAGNOSIS	$MF^{1^{st}}$	$DF^{1^{st}}_0$ ⓪	$[DF^{1^{st}}]$ ①	②	③	④	⑤	⑥	⑦	⑧	⑨	⑩	⑪	⑫	⑬	$\Delta P^{1^{st}}_s$
①	-1214	-1396	-	557	-24	-	-	1255	-	-486	-	6617	-34	-21	-	-
②	-450	-9	-	-	-80	-	-	-48	-	52	-	480	104	-	-	-
③	-	-	-	-	-	-	-	-	-	-	-	-	-	-	-	-
④	-	-	-	-	-	-	-	-	-	-	-	-	-	-	-	-
⑤	-	-	-	-	-	-	-	-	-	-	-	-	-	-	-	-
⑥	206	-12	-	-	-	-	-	-	-	-	-	-	-10	-	-	-
⑦	-	-	-	-	-	-	-	-	-	-	-	-	-	-	-	-
⑧	-136	-14	-	-	87	-	-	32	-	-23	-	-15	-25	-	-	-
⑨	-	-	-	-	-	-	-	-	-	-	-	-	-	-	-	-
⑩	1093	-	-	-	-	-	-	-	-	-	-	-	-	-	-	-
⑪	-40	-6	-	-	-	-	-	-	-	-	-	-	-	-	-	-
⑫	-1	-15	-	-	-	-	-	-	-	-	-	-	-	-	-	-129
⑬	-	-	-	-	-	-	-	-	-	-	-	-	-	-	-	-

- As was predicted, the components with higher malfunctions are those containing the anomalies (components HX, and RS; $MF^{1^{st}}_6 = 206\ MJ$ and $MF^{1^{st}}_{10} = 1093\ MJ$ repectively). However, these values are related to both intrinsic and induced malfunctions so *no immediate conclusions* can be extracted.
- This is also the reason why the other components exhibit non null values for the malfunctions ($MF^{1^{st}}_1 =- 1214\ MJ$; $MF^{1^{st}}_2 =- 450\ MJ$; $MF^{1^{st}}_8 =- 136\ MJ$; $MF^{1^{st}}_{11} =- 40\ MJ$ and $MF^{1^{st}}_{12} =- 1\ MJ$) due to the propagation of induced effects throughout the system which generates a $\Delta\kappa_i < 0$.
- As justified in [10], since the free condition is imposed, the faults produce less final product variation, $\Delta P^{1^{st}}_s < 0$. This fact influences each component's performance inducing a negative $\sum_i DF^{1^{st}}_{i,0} =- 1452\ MJ$.
- Mostly all malfunctions generate a local output variation; therefore, a dysfunction is created. The $DF^{1^{st}}_{i,j}$ matrix element exhibits the dysfunction part of ?? caused by a

malfunction in ??. The effects are commonly suffered by the components located upstream of the anomalies. Consequently, CB is the one undergoing the highest dysfunctions (sum of the 1st line): $DF_1^{1^{st}} = DF_{1,2}^{1^{st}} + DF_{1,3}^{1^{st}} + DF_{1,6}^{1^{st}} + DF_{1,10}^{1^{st}} + DF_{1,11}^{1^{st}} + DF_{1,12}^{1^{st}} = 7864\ MJ$.

- Conversely, RS is the component inducing the greatest dysfunction (sum of the 10th column): $DF_{1,10}^{1^{st}} + DF_{2,10}^{1^{st}} + DF_{6,10}^{1^{st}} + DF_{8,10}^{1^{st}} = 7082\ MJ$.
- The dysfunctions generated by HX $\left(\sum_i DF_{i,6}^{1^{st}} = 1239\ MJ\right)$ are also noticeable, but do not cause as much impact because they are located ahead in the supply chain.
- The existence of $\Delta P_{s_{DHW}}^{1^{st}} < 0$ is reflected in the last column.
- The sum of all components, according to eq(2), reflects the fuel impact related to the first diagnosis with three anomalies: $\Delta F_T^{1^{st}} = 6296\ MJ$.

Characteristic curves Diagnosis

Alternative analysis has been done considering the characteristic curves diagnosis methodology and has been applied hourly in every component. Subsequently, the values achieved as a result of the first analysis step are accumulated and depicted in Table 4. The column entitled as $\mathrm{MF}_{\mathrm{int}}^{1^{st}}$ contains the intrinsic malfunctions derived from anomalies, eq(16); the column $\mathrm{MF}_{\mathrm{ind}}^{1^{st}}$, alternatively , displays the induced malfunction due to the non-

Table 4: MF and DF first analysis step through characteristic curves

		CHARACTERISTIC CURVES		
		$\mathrm{MF}_{\mathrm{int}}^{1^{st}}$	$\mathrm{MF}_{\mathrm{ind}}^{1^{st}}$	$\mathrm{DF}^{1^{st}}$
①	CB	-	-1214	6467
②	HC	-	-450	500
③	D1	-	-	-
④	V1	-	-	-
⑤	M1	-	-	-
⑥	HX	323	-117	-22
⑦	V2	-	-	-
⑧	M2	-	-136	42
⑨	M3	-	-	-
⑩	RS	1212	-119	-
⑪	T	-	-40	-6
⑫	V3	-	-1	-15
⑬	D2	-	-	-

flat efficiency curves, eq(15). The sum of both columns indicates the total malfunction for each component. The last column remarks the dysfunction values obtained by eq(5).

- This procedure allows dividing and quantifying the induced malfunctions from the intrinsic ones. Henceforth, the results show clearly that the components with intrinsic malfunctions are $\left(MF^{1^{st}}_{6,int} = 323\ MJ\right)$ and $\left(MF^{1^{st}}_{10,int} = 1212\ MJ\right)$; therefore the components are HX and RS respectively.
- Nevertheless, this methodology does not permit one to identify the source of every component dysfunction, but only to calculate the total dysfunction $DF^{1^{st}}_{i}$ value.

Combination of both methods

As more than one intrinsic malfunction has taken place in the system, the subsystem with higher intrinsic malfunction can be recognized and identified as the faultiest component, in this case the RS. After erasing that anomaly, that is, restoring its reference energy performance, another simulation has been conducted in order to quantify the decrease of fuel impact accounted from the first study to the second one. In order to save space, the MF results of characteristic curves of the second analysis step are shown in Table 5,

Table 5: MF, DF and ΔPs analysis in the second analysis step

	CHARACTERISTIC CURVES		MF & *DF* DIAGNOSIS		
	$MF^{2^{nd}}_{int}$	$MF^{2^{nd}}_{ind}$	$DF^{2^{nd}}_{0}$	$DF^{2^{nd}}$	$\Delta P^{2^{nd}}_{s}$
① CB	-	-2048	-754	2197	-
② HC	-	-143	1	82	-
③ D1	-	-	-	-	-
④ V1	-	-	-	-	-
⑤ M1	-	-	-	-	-
⑥ HX	317	-118	-6	-9	-
⑦ V2	-	-	-	-	-
⑧ M2	-	-45	-11	59	-
⑨ M3	-	-	-	-	-
⑩ RS	-	18	-	-	-
⑪ T	-	-33	-12	-	-
⑫ V3	-	-1	-10	-	-76
⑬ D2	-	-	-	-	-

together with the DF, DF_0 and the final product vector taken from the other diagnosis analysis.

- In this 2nd case, as the anomaly in RS is corrected, only HX has intrinsic malfunctions, where $\left(MF^{2^{nd}}_{6,int} = 317\ MJ\right)$ outstands among all. Its value is slightly different to the one in the first study, owing to the reparation of the faultiest component that varies the faulty thermodynamic operation conditions.
- $DF^{2^{nd}}_{i,0}$ is again very remarkable. Indeed, as the fault is on the HX, the DHW final production is still lower than in the reference condition and that has an influence on the consumption reduction $\left(\sum_i DF^{2^{nd}}_{i,0} = -792\ MJ\right)$.
- In this case, as fewer anomalies are taken into account, $\Delta P_{s_{DHW}}^{2^{nd}}$ is closer to zero.
- The fuel impact related to the second diagnosis with one anomaly is: $\Delta F^{2^{nd}}_{T} = -590\ MJ$.

Therefore, it is in accordance with eq(17): $\Delta F_{save} = 6886\ MJ$.

So that, regarding eq(18), the induced malfunction generated by the anomaly in RS is equal to: $\sum_{10} MF^{1^{st}}_{10j,ind} = -695\ MJ$.

General results are summarized in Table 6 where each column corresponds to one of the anomalies deliberately inserted in the study and the rows MF_{int}, $\sum MF_{ind}$ and $\sum DF$ correspond to the intrinsic, induced malfunctions and dysfunctions the faulty components have in every study; the row $DF_0 + \Delta P_s$ indicates the effect the anomaly produces in the final production variation and its consequences. Finally, the $\Delta F_{anomaly}$ outlines the fuel impact of each anomaly.

Table 6: Diagnosis general results [MJ]

	RS' *anomaly*	HX' *anomaly*
MF_{int}	1212	317
$\sum MF_{ind}$	-695	-1270
$\sum DF$	7082	1230
$DF_0 + \Delta P_s$	-714	-867
$\Delta F_{anomaly}$	6886	-590

In this way the weight of fuel impact on each anomalous component can be attributed:

- The fault in RS generates an extra consumption of 6886 MJ where 7599 MJ are due to the fault itself and the remaining $-714\ MJ$ are owed to the final production decrease.
- The fault in HX generates an extra consumption of $-590\ MJ$ where 277 MJ are due to the fault itself and the remaining $-867\ MJ$ are owed to the final production decrease.

6. CONCLUSIONS AND DISCUSSION

The principle goal of the thermodynamic diagnosis of a system is the detection of the arising anomalies, the identification of the causes and the quantification of the effects.

Although diagnosis allows foreseeing possible breakdowns or preventing energy and economical extra charges, it has seldom been applied in *building thermal facilities*.

The main challenge of applying diagnoses to building thermal facilities is due to the need of the *dynamic representation* of the system. To do such type of analysis, hourly quasi-static states are joined together in order to typify the variable behaviour.

Henceforth, the productive structure of the system varies according to the component activation and deactivation. Besides the structure modifications, the independent variables of every component also change, so κ_i varies in each time-step as well. Therefore, the diagnosis methodologies should be calculated hourly and then the values obtained must be gathered until the end of the study period.

The *malfunction and dysfunction method* has been proved to be effective in evaluating malfunction effects, but appears to be ineffective in associating the extra consumption of the components with anomalies. In the case analysed in this paper, we conclude that it is not possible to signal the component where the intrinsic anomaly is present without a mathematical approach that separates it between intrinsic and malfunction analysis.

Conversely *characteristic curves* diagnosis methodology allows one to account for each component's *intrinsic* and *induced* malfunction on an individual basis.

While conventional diagnosis is achieved through the whole system *productive structure*, characteristic curves analysis is performed in each component individually.

The key finding is that neither of the methodologies is better than the other but they are complementary for a proper diagnosis. By means of the malfunction and dysfunction method, the fuel impact due to each malfunction can be accounted for and the one owing to the final production variation can be identified. Nonetheless, the method does not allow distinguishing between intrinsic and induced effects. On the contrary, the individual characteristic curves methodology allows us to differentiate them. By combining both theories, the fuel impact associated with each anomaly can be calculated through a reiterative diagnosis study.

Hence, the methodology allows studying components in a local way and learning how they affect globally. Hence, not only the efficiency degradation of the abnormal components are detected but also is accounted the extra fuel charge generated by each fault.

This theory is applied in a DHW and heating facility with two faults where RS is identified as the faultiest component. It provokes an overall extra consumption of $6886\ MJ$ during the heating period because of the incited effects on the others ($6387\ MJ$), the effects prompted in the component itself ($1212\ MJ$) and that are generated by changing the final production ($-714\ MJ$).

Acknowledments

The author, A Picallo, acknowledges the support provided to her by the Ministry of Education of the Spanish Government through a scholarship granted to her to complete her PhD degree. The authors also acknowledge the support provided by the Laboratory for the Quality Control in Buildings of the Basque Government.

REFERENCES

[1] Pérez-Lombard, L., Ortiz, J., & Pout, C. (2008). A review on buildings energy consumption information. Energy and Buildings, 40(3), 394-398.

[2] Piacentino, A., & Catrini, P. (2016). Assessing the Robustness of Thermoeconomic Diagnosis of Fouled Evaporators: Sensitivity Analysis of the Exergetic Performance of Direct Expansion Coils. Entropy, 18(3), 85

[3] Lozano, M. A., Bartolomé, J. L., Valero, A., & Reini, M. (1994). Thermoeconomic diagnosis of energy systems. In Flowers (Vol. 94, pp. 149-156).

[4] Torres, C., Valero, A., Serra, L., & Royo, J. (2002). Structural theory and thermoeconomic diagnosis: Part I. On malfunction and dysfunction analysis. Energy Conversion and Management, 43(9), 1503-1518.

[5] Toffolo, A., & Lazzaretto, A. (2007). A new thermoeconomic method for the location of causes of malfunctions in energy systems. Journal of Energy Resources Technology, 129(1), 1-9.

[6] Sciubba, E. (2001). Beyond thermoeconomics. The concept of extended exergy accounting and its application to the analysis and design of thermal systems. Exergy, an international journal, 1(2), 68-84.

[7] Torres, C., et al. (1996) The productive structure and thermoeconomic theories of system optimization. American Society of Mechanical Engineers, New York, NY (United States).

[8] Hepbasli, A. (2012). Low exergy (LowEx) heating and cooling systems for sustainable buildings and societies. Renewable and Sustainable Energy Reviews, 16(1), 73-104.

[9] Verda, V., Serra, L., & Valero, A. (2002). Thermoeconomic Diagnosis: Zooming Strategy Applied to Highly Complex Energy Systems—Part 2: On the Choice of the Productive Structure. In ASME 2002 International Mechanical Engineering Congress and Exposition (pp. 215-224). American Society of Mechanical Engineers.

[10] Picallo-Perez, A., Sala-Lizarraga, J. M., Iribar-Solabarrieta, E., & Odriozola-Maritorena, M. (2016) Application of the Malfunction Thermoeconomic Diagnosis to a Dynamic Heating and DHW Facility for Fault Detection. Energy and Buildings. 135, 385-397.

[11] Verda, V., Serra, L. M., & Valero, A. (2002). Zooming procedure for the thermoeconomic diagnosis of highly complex energy systems. International Journal of Thermodynamics, 5(2), 75-83.

[12] Verda, V., Serra, L., & Valero, A. (2004). The effects of the control system on the thermoeconomic diagnosis of a power plant. Energy, 29(3), 331-359.

[13] Mendes, T., Venturini, O. J., & Pirani, M. J. (2012). Thermodynamic Diagnosis Techniques To Assess The Behavior Of Vapour Compression Refrigeration Systems.

[14] Shi, Y., Xu, J., & Zhou, K. (2009). Structural theory and thermoeconomic diagnosis: application to a supercritical power plant. In 2009 Asia-Pacific Power and Energy Engineering Conference (pp. 1-4). IEEE.

[15] Piacentino, A., & Talamo, M. (2013). Innovative thermoeconomic diagnosis of multiple faults in air conditioning units: Methodological improvements and increased reliability of results. International Journal of Refrigeration, 36(8), 2343-2365.

[16] Piacentino, A., & Talamo, M. (2013). Critical analysis of conventional thermoeconomic approaches to the diagnosis of multiple faults in air conditioning units: capabilities, drawbacks and improvement directions. A case study for an air-cooled system with 120 kW capacity. International Journal of Refrigeration, 36(1), 24-44.

[17] Lazzaretto, A., & Toffolo, A. (2006). A critical review of the thermoeconomic diagnosis methodologies for the location of causes of malfunctions in energy systems. Journal of Energy Resources Technology, 128(4), 335-342.

[18] Reini, M., & Taccani, R. (2004). On the Thermoeconomic Approach to the Diagnosis of Energy System Malfunctions-The Role of the Fuel Impact Formula. International Journal of Thermodynamics, 7(2), 61-72.

[19] Picallo, A., Escudero, C., Flores, I., & Sala, J. M. (2016). Symbolic Thermoeconomics In Building Energy Supply Systems. Energy and Buildings, 127, 561-570.

[20] Valero, A., Correas, L., Zaleta, A., Lazzaretto, A., Verda, V., Reini, M., & Rangel, V. (2004). On the thermoeconomic approach to the diagnosis of energy system malfunctions: Part 2. Malfunction definitions and assessment. Energy, 29(12), 1889-1907.

[21] Usón, S., & Valero, A. (2007). Intrinsic and Induced Malfunctions Quantification in Thermoeconomic Diagnosis Through Quantitative Causality Analysis. Proceedings of ECOS 2007.

[22] Xu, J. Q., Yang, T., Zhou, K. Y., & Shi, Y. F. (2016). Malfunction diagnosis method for the thermal system of a power plant based on thermoeconomic analysis. Energy Sources, Part A: Recovery, Utilization, and Environmental Effects, 38(1), 124-132.

[23] Toffolo, A., & Lazzaretto, A. (2004). On the Thermoeconomic Approach to the Diagnosis of Energy System Malfunctions-Indicators to Diagnose Malfunctions: Application of a New Indicator for the Location of Causes. International Journal of Thermodynamics, 7(2), 41-49.

[24] Energy keys of the housing sector in the Basque Country. Claves energéticas del sector doméstico en Euskadi. EVE. (2013)

[25] Transient System Simulation Tool Trnsys, Thermal Energy Systems Specialists, Madison, USA.(2009)

[26] Lazzaretto, A., & Tsatsaronis, G. (2006). SPECO: a systematic and general methodology for calculating efficiencies and costs in thermal systems. Energy, 31(8), 1257-1289.